

Multi-channel Hybrid Access Femtocells: A Stochastic Geometric Analysis

Yi Zhong and Wenyi Zhang, *Senior Member, IEEE*

Abstract

For two-tier networks consisting of macrocells and femtocells, the channel access mechanism can be configured to be open access, closed access, or hybrid access. Hybrid access arises as a compromise between open and closed access mechanisms, in which a fraction of available spectrum resource is shared to nonsubscribers while the remaining reserved for subscribers. This paper focuses on a hybrid access mechanism for multi-channel femtocells which employ orthogonal spectrum access schemes. Considering a randomized channel assignment strategy, we analyze the performance in the downlink. Using stochastic geometry as technical tools, we derive the distributions of signal-to-interference-plus-noise ratios, and mean achievable rates, of both nonsubscribers and subscribers. The established expressions are amenable to numerical evaluation, and shed key insights into the performance tradeoff between subscribers and nonsubscribers. The analytical results are corroborated by numerical simulations.

Index Terms

Channel management, femtocell, hybrid access, spatial Poisson process, two-scale approximation, two-tier network

The authors are with Department of Electronic Engineering and Information Science, University of Science and Technology of China, Hefei 230027, China (email: geners@mail.ustc.edu.cn, wenyizha@ustc.edu.cn). The research has been supported by MIIT of China through grant 2011ZX03001-006-01 and by the Doctorial Program of Higher Education of China through grant 20103402120023.

I. INTRODUCTION

In current cellular network services, about 50% of phone calls and 70% of data services take place indoors [1]. For such indoor use cases, network coverage is a critical issue. One way to improve the indoor performance is to deploy the so-called femtocell access points (FAPs), also known as home base stations, besides macrocell base stations (MBSs). Femtocells are small cellular base stations, typically designed for use in home or small business [2][3]. The use of femtocells not only benefits the users, but also the operators. As the distance between the transmitter and receiver is reduced, users will enjoy high quality links and power savings. Furthermore, the reduced transmission range also creates more spatial reuse and reduces electromagnetic interference.

Among the many challenges faced by femtocells, and more generally, two-tier networks, is the issue of interference; see Figure 1. The two-tier interference problem differs from that in traditional single-tier networks in several important aspects: First, due to the limitations of access mechanism, a user equipment (UE) may not be able to connect to the access point which offers the best service. Second, since femtocells connect to operator's core network via subscribers' private ISP, coordination between macrocells and femtocells and among femtocells is limited. Finally, compared to planned macrocell deployments, femtocells are usually deployed in an ad hoc manner, and the thus randomly placed femtocells make it difficult to manage the interference. In two-tier networks comprising of macrocells and femtocells, interference can be categorized into two types:

- **Cross-tier:** This refers to the interference from one tier to the other; that is, femtocell interference at a macrocell and macrocell interference at a femtocell.
- **Co-tier:** This refers to the interference within a tier; that is, femtocell interference at a nearby femtocell and macrocell interference at a nearby macrocell.

In this paper, we consider two-tier networks that are based on multicarrier techniques, for example those deploying LTE or WiMAX standards, which use orthogonal frequency-division multiple access (OFDMA) techniques. In multicarrier systems, the available spectrum is divided into orthogonal subcarriers, which are then grouped into multiple subchannels, assigned to different users. Due to the flexibility in channel assignment, both cross-tier and co-tier interferences may be alleviated.

The access mechanism of femtocells (see, e.g., [4]) is a key factor that affects the performance of two-tier networks, and generally can be classified as follows, where we call the UEs that register to a femtocell as subscribers, and those that do not register to any femtocell as nonsubscribers.

- **Closed access:** An FAP only allows its subscribers to connect.
- **Open access:** An FAP allows all its covered UEs, no matter registered or not, to connect.
- **Hybrid access:** An FAP allows its covered nonsubscribers to connect via a subset of its available subchannels, and reserves the remaining subchannels for its subscribers.

Hybrid access [5] is an intermediate approach, in which a fraction of the total available resource is allocated to nonsubscribers. By doing so, nonsubscribers near an FAP may handover into the femtocell to avoid high interference; meanwhile, with a certain amount of resource reserved for subscribers, the performance of subscribers may be well assured even in the presence of nonsubscribers.

In hybrid access, a central issue is how to allocate the resource between subscribers and nonsubscribers. Previous studies [6] [7] indicate that hybrid access improves the network performance at the cost of reduced performance for subscribers, therefore suggesting a tradeoff between the performance of nonsubscribers and subscribers. In this paper, we consider a hybrid access mechanism that uses a randomized channel assignment strategy, and analyze the performance in the downlink of both macrocells and femtocells. We employ stochastic geometry to characterize the spatial distributions of users as well as access points; see, e.g., [8] and references therein for its recent applications in wireless networks. Accordingly, we derive the key performance indicators including blocking probabilities, mean achievable rates, and distributions of the signal-to-interference-plus-noise ratios (SINRs), of both nonsubscribers and subscribers. In our study, we establish general integral expressions for the performance indicators, and closed form expressions under specific model parameters. With the obtained results, we reveal how the performance of subscribers and nonsubscribers trades off each other.

An overview of related works is as follows. In [9], the authors proposed to study key performance indicators for cellular networks, such as coverage probabilities and mean achievable rates, through models and tools in stochastic geometry. Our work explores that approach in hybrid access femtocell networks, focusing on multi-channel models and the downlink performance. In [10], the considered scheme divides the spectrum resource into two orthogonal parts which are

assigned to macrocells and femtocells, respectively, with femtocells being closed access. In [11], the authors considered two-tier femtocell networks using time-hopped CDMA, examining the uplink outage probability and the interference avoidance capability. In [12] and [13], the authors studied the performance of various femtocell access mechanisms, under substantially different system models from ours. Our work examines the interaction among multiple MBSs and FAPs, and focuses on scenarios in which macrocells and femtocells share the same frequency band, following a hybrid access mechanism, as will be elaborated in Section II.

The remaining part of the paper is organized as follows. Section II describes the two-tier network model, the channel assignment strategy, and the hybrid access mechanism. Based on a two-scale approximation for the spatial distributions of femtocells, Section III analyzes the statistical behavior of UEs, deriving the distributions of the number of UEs connecting to either an FAP or an MBS, as well as the probabilities of a subchannel being used by either an FAP or an MBS. Built upon those statistics, Section IV establishes expressions for the distributions of the SINRs, and the mean achievable rates. Section V illustrates the aforementioned analysis by numerical results, which are also corroborated by simulations. Finally, Section VI concludes the paper.

II. NETWORK MODEL

A. Hybrid Access Femtocells

In the two-tier network, we consider two types of access points, MBSs and FAPs. The MBSs constitute the macrocell tier, and they induce a Voronoi tessellation of the plane (see Figure 2). When a UE attempts to access the macrocell network, it chooses to connect to the MBS in the Voronoi cell which it is situated in. An FAP provides network access to UEs in its vicinity, and we assume that all FAPs have a covering radius of R_f . Within the covered circular area of each FAP are two types of UEs, called subscribers and inside nonsubscribers. Inside nonsubscribers are those UEs who gather around an FAP without subscribing to its service; for example, transient customers in a shop or restaurant. Besides those two types of UEs, we also consider a third type of UEs, outside nonsubscribers, who are uniformly scattered over the whole plane, corresponding to those regular macrocell network users.

The available spectrum is evenly divided into M subchannels, which are to be shared by both the macrocell tier and the femtocell tier. Each FAP is configured to allocate a fixed number, M_s ,

of subchannels for its covered inside nonsubscribers. These M_s subchannels are called shared subchannels, and the remaining $M_r = M - M_s$ subchannels are called reserved subchannels as they are reserved for the subscribers. In the considered hybrid access mechanism, each FAP selects its shared subchannels randomly, and independently of other FAPs. We assume that each UE, whether subscriber or nonsubscriber, needs one subchannel for accessing the two-tier network. When a UE accessing an MBS or an FAP, the serving subchannel is selected randomly (see Figure 3).

The hybrid access mechanism operates as follows.

- A subscriber accesses to one of the M_r reserved subchannels of its corresponding FAP. When there are more than M_r subscribers in an FAP, they are served by time-sharing with equal time proportion.
- An inside nonsubscriber accesses to one of the M_s shared subchannels of its covering FAP. When there are more than M_s inside nonsubscribers in an FAP, they are served by time-sharing with equal time proportion.
- An outside nonsubscriber accesses the MBS in the Voronoi cell which the outside nonsubscriber is situated in. When there are more than M outside nonsubscribers in the Voronoi cell, they are served by time-sharing with equal proportion.

B. Mathematical Model and Two-scale Approximation

To formulate the aforementioned hybrid access scenario mathematically, we model the spatial distributions of the nodes using spatial Poisson processes as follows. The MBSs constitute a homogeneous Poisson point process (PPP) Φ_m of intensity λ_m on the plane; the FAPs constitute another homogeneous PPP Φ_f of intensity λ_f . In the circular covered area of radius R_f of each FAP, the subscribers are distributed according to a homogeneous PPP of intensity λ_s , and the inside nonsubscribers are distributed according to another homogeneous PPP of intensity λ_{in} . Outside nonsubscribers constitute on the whole plane a homogeneous PPP of intensity λ_{out} . All the PPPs are mutually independent.

In this paper, we focus on the downlink performance. The transmit power is set to a constant value P_m for an MBS, and P_f for an FAP. For the sake of convenience, we adopt a standard path loss propagation model with path loss exponent $\alpha > 2$. Regarding fading, we assume that the link between the serving access point (either an MBS or an FAP) and the served UE experiences

Rayleigh fading with parameter μ . The received signal power of a UE at a distance r from its serving access point therefore is $P_m hr^{-\alpha}$ (MBS) or $P_f hr^{-\alpha}$ (FAP) where $h \sim \text{Exp}(\mu)$. The fading of interference links may follow an arbitrary probability distribution, and is denoted by g . Furthermore, considering the typical scenario of indoor femtocell deployment, we introduce a wall isolation at the boundary of each FAP coverage area, which incurs a wall penetration loss factor $W < 1$. For all receivers, the noise power is σ^2 .

The different PPPs corresponding to different entities in the network interact in a complicated way, thus making a rigorous statistical analysis extremely difficult. For example, an inside nonsubscriber may be covered by more than one FAPs, thus leading to the delicate issue of FAP selection, and furthermore rendering the subchannel usage distributions among FAPs and MBSs intrinsically correlated. To overcome the technical difficulties due to spatial interactions, in the subsequent analysis we propose a two-scale approximation for the network model, motivated by the fact that the covered area of an FAP is significantly smaller than that of an MBS. The two-scale approximation consists of two views, the macro-scale view and the micro-scale view. The macro-scale view concerns an observer outside the coverage area of an FAP, and in that view the whole coverage area of the FAP shrinks to a single point, marked by the numbers of subscribers and inside nonsubscribers therein. The micro-scale view concerns an observer inside the coverage area of an FAP, and in that view the coverage area is still circular with radius R_f in which the subscribers and inside nonsubscribers are spatially distributed. By such a two-scale approximation, an inside nonsubscriber can only be covered by a unique FAP, and the coverage area of an FAP can only be within a unique Voronoi cell of an MBS. These consequences substantially simplify the performance analysis. In Section V, we validate the two-scale approximation method through comparing analytical results and simulation results, for network parameters of practical interest.

III. STATISTICS OF UES AND SUBCHANNELS

In this section, we characterize the distributions of UEs connecting to different types of access points, and the distributions of used subchannels in MBSs and FAPs. The analysis is based on a snapshot of the network model, and the obtained results will then be applied for characterizing the distributions of SINRs and achievable rates in Section IV.

A. Distributions of UEs

Let U_s be the number of subscribers accessing a given FAP and from our model we have $U_s \sim \text{Poisson}(\lambda_s \pi R_f^2)$. Similarly, let U_{in} be the number of inside nonsubscribers accessing a given FAP, and we have $U_{\text{in}} \sim \text{Poisson}(\lambda_{\text{in}} \pi R_f^2)$.

The number of outside nonsubscribers who access a given MBS, denoted by U_{out} , is characterized as follows. We note that the macrocell coverage area is a Voronoi cell, and denote by S the area of the Voronoi cell. There is no known closed form expression of the probability density function (pdf) of S , whereas a simple approximation [14] has proven sufficiently accurate for practical purposes. Considering scaling, the approximate pdf of the size of a macrocell coverage area is given by

$$f(S) = \frac{343}{15} \sqrt{\frac{7}{2\pi}} (S\lambda_m)^{\frac{5}{2}} \exp\left(-\frac{7}{2}S\lambda_m\right)\lambda_m. \quad (1)$$

Conditioned upon S , the number of outside nonsubscribers is a Poisson random variable with mean $\lambda_{\text{out}}S$. The probability generating function (pgf) of the unconditioned U_{out} is thus given by

$$G(z) = \int_0^\infty \exp\left(\lambda_{\text{out}}(z-1)S\right) f(S) dS. \quad (2)$$

Plugging in the approximate pdf of S and simplifying the integral, we get

$$G(z) = \frac{343}{8} \sqrt{\frac{7}{2}} \left(\frac{7}{2} - \frac{\lambda_{\text{out}}}{\lambda_m}(z-1)\right)^{-\frac{7}{2}}. \quad (3)$$

The distribution of U_{out} is therefore given by the derivatives of $G(z)$,

$$\mathbb{P}\{U_{\text{out}} = i\} = \frac{G^{(i)}(0)}{i!}, \quad i = 0, 1, \dots \quad (4)$$

B. Distributions of Subchannel Usage

Since the subchannels are uniformly and independently selected by each FAP, it suffices to analyze an arbitrary one of them. Let us examine the probability that a given subchannel is used by an MBS or an FAP. In order to obtain the probability, we evaluate the average number of subchannels used by an MBS or an FAP, and then normalize the average number by the total number of subchannels, M .

The probability that a subchannel is used by an FAP is

$$\begin{aligned}
P_{\text{busy},f} &= \frac{1}{M} \left(\sum_{i=0}^{\infty} \min\{i, M_r\} \mathbb{P}\{U_s = i\} + \sum_{j=0}^{\infty} \min\{j, M_s\} \mathbb{P}\{U_{\text{in}} = j\} \right) \\
&= \frac{1}{M} \sum_{i=0}^{M_r} i \mathbb{P}\{U_s = i\} + \left(1 - \frac{M_s}{M}\right) \sum_{i=M_r+1}^{\infty} \mathbb{P}\{U_s = i\} + \\
&\quad + \frac{1}{M} \sum_{j=0}^{M_s} j \mathbb{P}\{U_{\text{in}} = j\} + \frac{M_s}{M} \sum_{j=M_s+1}^{\infty} \mathbb{P}\{U_{\text{in}} = j\}. \tag{5}
\end{aligned}$$

For a Poisson random variable $N \sim \text{Poisson}(\lambda)$, its cumulative distribution function (cdf) is given by

$$\sum_{i=0}^n \mathbb{P}\{N = i\} = \sum_{i=0}^n \frac{\lambda^i}{i!} e^{-\lambda} = \frac{\Gamma(n+1, \lambda)}{n!}, \tag{6}$$

where $\Gamma(s, x) = \int_x^{\infty} t^{s-1} e^{-t} dt$ is the incomplete gamma function. Using (6) to simplify $P_{\text{busy},f}$, we get

$$\begin{aligned}
P_{\text{busy},f} &= 1 + \frac{M_r}{M} \frac{1}{M_r!} \left(\lambda_s \pi R_f^2 \Gamma(M_r, \lambda_s \pi R_f^2) - \Gamma(M_r + 1, \lambda_s \pi R_f^2) \right) + \\
&\quad + \frac{M_s}{M} \frac{1}{M_s!} \left(\lambda_{\text{in}} \pi R_f^2 \Gamma(M_s, \lambda_{\text{in}} \pi R_f^2) - \Gamma(M_s + 1, \lambda_{\text{in}} \pi R_f^2) \right). \tag{7}
\end{aligned}$$

The probability that a subchannel is used by an MBS is

$$P_{\text{busy},m} = \frac{1}{M} \sum_{i=0}^{\infty} \min\{i, M\} \mathbb{P}\{U_{\text{out}} = i\}, \tag{8}$$

where $\mathbb{P}\{U_{\text{out}} = i\}$ is given by (4).

The spatial process of FAPs that use a given subchannel is the independent thinning of the original PPP of FAPs Φ_f by the probability $P_{\text{busy},f}$, denoted by Φ'_f with intensity $\lambda'_f = \lambda_f P_{\text{busy},f}$. The term ‘‘independent thinning’’ means that Φ'_f can be viewed as obtained from Φ_f by independently removing points with probability $1 - P_{\text{busy},f}$. Similarly, the spatial process of MBSs that use a given subchannel is the independent thinning of the original PPP of MBSs Φ_m by the probability $P_{\text{busy},m}$, denoted by Φ'_m with intensity $\lambda'_m = \lambda_m P_{\text{busy},m}$. These two independently thinned PPPs will prove useful in the subsequent analysis.

IV. ANALYSIS OF SINR AND MEAN ACHIEVABLE RATE

In this section, we derive the distributions of SINRs and the mean achievable rates of all the three types of UEs. For each type of UEs, we begin with general settings, and then simplify the

general results under several specific parameters to gain insights. The mean achievable rates are the averaged instantaneous achievable rates over both channel fading and spatial distributions of UEs and access points.

A. Macrocell UEs

1) *General Case:* For an active UE served by an MBS, it must be occupying one subchannel of the MBS. The following theorem gives the cdf of SINR and the mean achievable rate of each active macrocell UE in general case.

Theorem 1: The cdf of the SINR of a macrocell UE, denoted by $Z_m(T) = \mathbb{P}\{\text{SINR} \leq T\}$, is given by

$$Z_m(T) = 1 - \pi \lambda_m \int_0^\infty \exp\left(\pi v \lambda'_m \left(1 - \beta(T, \alpha) - \frac{1}{P_{\text{busy},m}}\right) - \frac{\mu T v^{\frac{\alpha}{2}} \sigma^2}{P_m}\right) dv. \quad (9)$$

The mean achievable rate of a macrocell UE is given by

$$\tau_m = \pi \lambda_m \int_0^\infty \int_0^\infty \exp\left(\pi v \lambda'_m \left(1 - \beta(e^t - 1, \alpha) - \frac{1}{P_{\text{busy},m}}\right) - \frac{\mu v^{\frac{\alpha}{2}} \sigma^2 (e^t - 1)}{P_m}\right) dt dv. \quad (10)$$

In (9) and (10), $\beta(T, \alpha)$ is given by

$$\beta(T, \alpha) = \frac{2(\mu T)^\frac{2}{\alpha}}{\alpha} \mathbb{E}_g \left(g^\frac{2}{\alpha} \left(\Gamma\left(-\frac{2}{\alpha}, \mu T g\right) - \left(1 + \frac{\lambda'_f (W P_f)^\frac{2}{\alpha}}{\lambda'_m P_m^\frac{2}{\alpha}}\right) \Gamma\left(-\frac{2}{\alpha}\right) \right) \right). \quad (11)$$

The proof of Theorem 1 is in Appendix A.

In Theorem 1, $Z_m(T)$ in (9) gives the probability that the SINR is below a given target level T , and τ_m in (10) gives the mean achievable rate of a macrocell UE. The integrals in (9) and (10) can be evaluated by numerical methods, and furthermore, they can be simplified to concise forms in a number of special cases. The cases of interest in this paper are the combinations of (i) interference experiencing Rayleigh fading, (ii) the path loss exponent being $\alpha = 4$, and (iii) no noise or the noise is weak, $\sigma^2 \rightarrow 0$. The following discussions are categorized into two parts according to the interference fading.

2) *Special Case When Interference Experiences General Fading:*

a) *General Fading, Noise, $\alpha = 4$:* We can simplify (9) via invoking the identity

$$\int_0^\infty e^{-ax} e^{-bx^2} dx = \sqrt{\frac{\pi}{b}} \exp\left(\frac{a^2}{4b}\right) Q\left(\frac{a}{\sqrt{2b}}\right), \quad (12)$$

where $Q(x) = \frac{1}{\sqrt{2\pi}} \int_x^\infty \exp(-y^2/2) dy$ is the standard Gaussian tail probability. Letting $a(T) = \pi\lambda'_m(\beta(T, 4) + \lambda_m/\lambda'_m - 1)$, we have

$$Z_m(T) = 1 - \pi\lambda_m \sqrt{\frac{\pi P_m}{\mu T \sigma^2}} \exp\left(\frac{a^2(T) P_m}{4\mu T \sigma^2}\right) Q\left(a(T) \sqrt{\frac{P_m}{2\mu T \sigma^2}}\right). \quad (13)$$

For a given distribution of interference fading, $\beta(T, 4)$ can be evaluated by numeric methods, and subsequently the SINR distribution $Z_m(T)$ can be obtained conveniently.

b) General Fading, Small Noise, $\alpha > 2$: Consider the interference-limited regime in which the noise power is approaching zero. Using the expansion $e^{-x} = 1 - x + o(x)$ as $x \rightarrow 0$, the SINR distribution behaves like

$$Z_m(T) = 1 - \frac{1}{1 + (\beta(T, \alpha) - 1) P_{\text{busy},m}} + \frac{\pi\lambda_m \mu T \sigma^2 \Gamma(\alpha/2 + 1)}{\left(\pi\lambda'_m (\beta(T, \alpha) + \lambda_m/\lambda'_m - 1)\right)^{\alpha/2+1} P_m} + o(\sigma^2). \quad (14)$$

When $\sigma^2 = 0$, the SINR distribution is further simplified into

$$Z_m(T) = 1 - \frac{1}{1 + (\beta(T, \alpha) - 1) P_{\text{busy},m}}. \quad (15)$$

3) Special Case When Interference Experiences Rayleigh Fading: Here we consider the case where the interference experiences Rayleigh fading with mean μ , i.e. $g \sim \text{Exp}(\mu)$. In this case, the results are simplified as follows.

Corollary 1: When the interference follows Rayleigh fading, the cdf of the SINR is

$$Z_m(T) = 1 - \pi\lambda_m \int_0^\infty \exp\left(-\pi v \lambda_m - \pi v \lambda'_m \varphi(T, \alpha, T^{-2/\alpha}) - \pi v \lambda'_f \varphi\left(\frac{P_f W T}{P_m}, \alpha, 0\right) - \frac{\mu T v^{\alpha/2} \sigma^2}{P_m}\right) dv. \quad (16)$$

The mean achievable rate is

$$\tau_m = \pi\lambda_m \int_0^\infty \int_0^\infty \exp\left(-\pi v \lambda_m - \pi v \lambda'_m \varphi\left(e^t - 1, \alpha, (e^t - 1)^{-2/\alpha}\right) - \pi v \lambda'_f \varphi\left(\frac{P_f W (e^t - 1)}{P_m}, \alpha, 0\right) - \frac{\mu v^{\alpha/2} \sigma^2 (e^t - 1)}{P_m}\right) dv dt, \quad (17)$$

where

$$\varphi(T, \alpha, x) = T^{2/\alpha} \int_x^\infty \frac{1}{1 + u^{\alpha/2}} du. \quad (18)$$

The results in Corollary 1 are further simplified in the following special cases.

a) *Rayleigh Fading, Noise*, $\alpha = 4$: Using (12), we get

$$Z_m(T) = 1 - \pi\lambda_m \sqrt{\frac{\pi P_m}{\mu T \sigma^2}} \exp\left(\frac{\kappa^2(T) P_m}{4\mu T \sigma^2}\right) Q\left(\kappa(T) \sqrt{\frac{P_m}{2\mu T \sigma^2}}\right). \quad (19)$$

The mean achievable rate of a macrocell UE is simplified into

$$\tau_m = \pi\lambda_m \int_0^\infty \sqrt{\frac{\pi P_m}{\mu \sigma^2 (e^t - 1)}} \exp\left(\frac{\kappa^2(e^t - 1) P_m}{4\mu \sigma^2 (e^t - 1)}\right) Q\left(\kappa(e^t - 1) \sqrt{\frac{P_m}{2\mu \sigma^2 (e^t - 1)}}\right) dt, \quad (20)$$

where

$$\kappa(T) = \pi\lambda_m + \pi\lambda'_m \sqrt{T} (\pi/2 - \arctan \sqrt{T}) + \frac{\pi^2 \lambda'_f}{2} \sqrt{\frac{P_f W T}{P_m}}. \quad (21)$$

b) *Rayleigh Fading, No Noise*, $\alpha > 2$: When $\sigma^2 = 0$, the SINR distribution is simplified into

$$Z_m(T) = 1 - \frac{1}{1 + \frac{\lambda'_m}{\lambda_m} \varphi(T, \alpha, T^{-2/\alpha}) + \frac{\lambda'_f}{\lambda_m} \varphi\left(\frac{P_f W T}{P_m}, \alpha, 0\right)}. \quad (22)$$

The mean achievable rate of a macrocell UE is simplified into

$$\tau_m = \int_0^\infty \frac{1}{1 + \frac{\lambda'_m}{\lambda_m} \varphi(e^t - 1, \alpha, (e^t - 1)^{-2/\alpha}) + \frac{\lambda'_f}{\lambda_m} \varphi\left(\frac{P_f W (e^t - 1)}{P_m}, \alpha, 0\right)} dt. \quad (23)$$

Specifically, when $\alpha = 4$ we obtain

$$Z_m(T) = 1 - \frac{1}{1 + \sqrt{T} \left(\frac{\pi}{2} - \arctan \sqrt{T} + \frac{\pi}{2} \frac{\lambda'_f}{\lambda'_m} \sqrt{\frac{W P_f}{P_m}} \right) P_{\text{busy},m}}. \quad (24)$$

The mean achievable rate of a macrocell UE is simplified into

$$\tau_m = \int_0^{\pi/2} \frac{2}{\tan y + (\pi/2 - y) P_{\text{busy},m} + \frac{\pi}{2} \frac{\lambda'_f}{\lambda'_m} \sqrt{\frac{W P_f}{P_m}}} dy. \quad (25)$$

From a practical perspective, it is desirable to shape $Z_m(T)$ to make it small for small values of T . From (24), we see that there are two approaches to shape $Z_m(T)$. First, $Z_m(T)$ decreases as $P_{\text{busy},m}$, the probability that a subchannel is used by an MBS, decreases. This may be interpreted as an effect of frequency reuse. Second, $Z_m(T)$ decreases as the whole term, $\frac{\lambda'_f}{\lambda'_m} \sqrt{\frac{W P_f}{P_m}}$, decreases, which corresponds to a number of network parameters, representing the effect due to the deployment of the femtocell tier.

B. Femtocell UEs

1) *General Case*: A UE served by an FAP occupies one subchannel of the FAP. The following theorem gives the cdf of SINR and the mean achievable rate of each active femtocell UE in general case.

Theorem 2: The cdf of the SINR of a femtocell UE in general case is given by

$$Z_f(T) = 1 - \frac{1}{R_f^2} \int_0^{R_f^2} \exp\left(-\rho(\alpha)T^{2/\alpha}v - \frac{\mu T v^{\alpha/2} \sigma^2}{P_f}\right) dv. \quad (26)$$

The mean achievable rate of a femtocell UE is given by

$$\tau_f = \frac{1}{R_f^2} \int_0^{R_f^2} \int_0^\infty \exp\left(-\rho(\alpha)(e^t - 1)^{2/\alpha}v - \frac{\mu v^{\alpha/2} \sigma^2 (e^t - 1)}{P_f}\right) dt dv. \quad (27)$$

in (26) and (27), $\rho(\alpha)$ is given by

$$\rho(\alpha) = -\frac{2\pi\mu^{2/\alpha}}{\alpha} \Gamma\left(-\frac{2}{\alpha}\right) \left(\lambda'_m \left(\frac{WP_m}{P_f}\right)^{2/\alpha} + \lambda'_f W^{4/\alpha}\right) \mathbb{E}_g(g^{2/\alpha}). \quad (28)$$

The proof of Theorem 2 is in Appendix B.

2) Special Case When Interference Experiences General Fading:

a) *General Fading, Noise, $\alpha = 4$* : Using the following identity to simplify the results in Theorem 2,

$$\int_0^u e^{-ax} e^{-bx^2} dx = \sqrt{\frac{\pi}{b}} \exp\left(\frac{a^2}{4b}\right) \left(\text{Q}\left(\frac{a}{\sqrt{2b}}\right) - \text{Q}\left(\frac{a}{\sqrt{2b}} - u\sqrt{b}\right)\right), \quad (29)$$

we get the SINR distribution as

$$Z_f(T) = 1 - \frac{1}{R_f^2} \sqrt{\frac{\pi P_f}{\mu T \sigma^2}} \exp\left(\frac{\rho^2(4)P_f}{4\mu\sigma^2}\right) \left(\text{Q}\left(\rho(4)\sqrt{\frac{P_f}{2\mu\sigma^2}}\right) - \text{Q}\left(\rho(4)\sqrt{\frac{P_f}{2\mu\sigma^2}} - R_f^2 \sqrt{\frac{\mu\sigma^2 T}{P_f}}\right)\right). \quad (30)$$

The mean achievable rate is simplified into

$$\tau_f = \frac{1}{R_f^2} \sqrt{\frac{\pi P_f}{\mu\sigma^2}} \exp\left(\frac{\rho^2(4)P_f}{4\mu\sigma^2}\right) \int_0^\infty \psi(t) dt, \quad (31)$$

where

$$\psi(t) = \frac{1}{\sqrt{e^t - 1}} \left(\text{Q}\left(\rho(4)\sqrt{\frac{P_f}{2\mu\sigma^2}}\right) - \text{Q}\left(\rho(4)\sqrt{\frac{P_f}{2\mu\sigma^2}} - R_f^2 \sqrt{\frac{\mu\sigma^2(e^t - 1)}{P_f}}\right)\right).$$

b) *General Fading, Small Noise, $\alpha > 2$* : As the noise power is approaching zero, we have

$$Z_f(T) = 1 - \frac{1 - e^{-\rho(\alpha)T^{2/\alpha}R_f^2}}{\rho(\alpha)T^{2/\alpha}R_f^2} + \frac{\mu\sigma^2 R_f^\alpha (\Gamma(1 + \frac{\alpha}{2}) - \Gamma(1 + \frac{\alpha}{2}, R_f^2))}{P_f[\rho(\alpha)]^{\alpha/2+1}T^{\alpha/2}} + o(\sigma^2). \quad (32)$$

When $\sigma^2 = 0$, we further get

$$Z_f(T) = 1 - \frac{1 - e^{-\rho(\alpha)T^{2/\alpha}R_f^2}}{\rho(\alpha)T^{2/\alpha}R_f^2}, \quad (33)$$

and the mean achievable rate is

$$\tau_f = \frac{1}{\rho(\alpha)R_f^2} \int_0^\infty \frac{1 - e^{-\rho(\alpha)(e^t-1)^{2/\alpha}R_f^2}}{(e^t-1)^{2/\alpha}} dt. \quad (34)$$

3) *Special Case When Interference Experiences Rayleigh Fading*: For Rayleigh fading, the results are essentially the same as that in the general fading case. The only additional simplification is the evaluation of $\rho(\alpha)$. We just give the result in the very special case when $\sigma^2 = 0$ and $\alpha = 4$.

When the interference experiences Rayleigh fading, we have $\mathbb{E}_g(g^{\frac{1}{2}}) = \mu \int_0^\infty g^{\frac{1}{2}} e^{-\mu g} dg = (1/2) \cdot \sqrt{\pi/\mu}$, and consequently,

$$\rho(4) = \frac{\pi^2}{2} \left(\lambda'_m \sqrt{\frac{WP_m}{P_f}} + \lambda'_f W \right). \quad (35)$$

The SINR distribution is then given by

$$Z_f(T) = 1 - \frac{1 - e^{-\rho(4)\sqrt{T}R_f^2}}{\rho(4)\sqrt{T}R_f^2}. \quad (36)$$

The mean achievable rate is simplified into

$$\begin{aligned} \tau_f &= \int_0^\infty \frac{1 - e^{-\rho(4)R_f^2\sqrt{e^t-1}}}{\rho(4)R_f^2\sqrt{e^t-1}} dt \\ &= 2 \int_0^\infty \frac{1 - e^{-y}}{y^2 + \rho^2(4)R_f^4} dy. \end{aligned} \quad (37)$$

These expressions are convenient for numerical evaluation.

C. Mean Achievable Rates of Nonsubscribers and Subscribers

There are two types of nonsubscribers: those outside nonsubscribers who access MBSs and those inside nonsubscribers who access FAPs. When the number of outside nonsubscribers in a macrocell is no greater than the total number of subchannels (i.e., $U_{\text{out}} \leq M$), each nonsubscriber

UE exclusively occupies a subchannel, and its mean achievable rate is τ_m . However, when $U_{\text{out}} > M$, those U_{out} UEs share the M subchannels with mean achievable rate $\frac{M}{U_{\text{out}}}\tau_m$. Since the evaluation is conditioned upon the existence of at least one UE, the mean achievable rate of an outside nonsubscriber UE is given by

$$\tau_{\text{out}} = \frac{\sum_{i=1}^M \mathbb{P}\{U_{\text{out}} = i\} + \sum_{i=M+1}^{\infty} \mathbb{P}\{U_{\text{out}} = i\} \frac{M}{i}}{1 - \mathbb{P}\{U_{\text{out}} = 0\}} \tau_m. \quad (38)$$

Similarly, the mean achievable rate of an inside nonsubscriber is given by

$$\tau_{\text{in}} = \frac{\sum_{j=1}^{M_s} \mathbb{P}\{U_{\text{in}} = j\} + \sum_{j=M_s+1}^{\infty} \mathbb{P}\{U_{\text{in}} = j\} \frac{M_s}{j}}{1 - \mathbb{P}\{U_{\text{in}} = 0\}} \tau_f. \quad (39)$$

When averaged over both inside and outside nonsubscribers, the overall mean achievable rate of nonsubscriber is obtained as

$$\tau_n = \frac{\lambda_{\text{out}}\tau_{\text{out}} + \lambda_f\lambda_{\text{in}}\pi R_f^2\tau_{\text{in}}}{\lambda_{\text{out}} + \lambda_f\lambda_{\text{in}}\pi R_f^2}. \quad (40)$$

Regarding subscribers, note that they are exclusively served by FAPs. Similar to the analysis of nonsubscribers, the mean achievable rate of a subscriber is given by

$$\tau_s = \frac{\sum_{i=1}^{M_r} \mathbb{P}\{U_s = i\} + \sum_{i=M_r+1}^{\infty} \mathbb{P}\{U_s = i\} \frac{M_r}{i}}{1 - \mathbb{P}\{U_s = 0\}} \tau_f. \quad (41)$$

V. NUMERICAL RESULTS

The numerical results are obtained according to both the analytical results we have derived and Monte Carlo simulation. The default configurations of system model are as follows (also see Table I). The total number of subchannels is $M = 20$ and the coverage radius of each femtocell is $R_f = 10\text{m}$. The transmit power of an FAP is set as $P_f = 13\text{dBm}$ and that of an MBS $P_m = 39\text{dBm}$. We set the path loss exponent as $\alpha = 4$, with all links experiencing Rayleigh fading of normalized $\mu = 1$. The wall penetration loss is set as $W = -6\text{dB}$. We focus on the interference-limited regime, and for simplicity we ignore the noise power (i.e., $\sigma^2 = 0$). The density of MBSs is set as $\lambda_m = 0.00001$ and of FAPs $\lambda_f = 0.0001$. So the average coverage area of an MBS is roughly equal to a circle with a radius of 180m, and on average there are ten FAPs within the coverage area of an MBS. Unless otherwise specified, the subscribers and inside nonsubscribers are distributed within an FAP coverage area with intensities $\lambda_s = \lambda_{\text{in}} = 0.015$. The intensity of outside nonsubscribers is set as $\lambda_{\text{out}} = 0.0001$. So on average, each femtocell contains about 10 subscribers and inside nonsubscribers, and each macrocell contains about

10 outside nonsubscribers. Note that due to statistical fluctuations, the number of UEs may occasionally exceeds the number of available subchannels.

Figure 4 displays the SINR distributions of macrocell UEs and femtocell UEs, when the number of shared subchannels is set as $M_s = 10$. We plot in dotted curves the analytical results, and we also plot the empirical cdfs obtained from Monte Carlo simulation. The curves reveal that the simulation results match the analytical results well, thus corroborating the accuracy of our theoretical analysis. From the SINR distributions, we observe that while the macrocell UEs experience a fair amount of interference, due to the shrinking cell size, the interference for femtocell UEs is substantially alleviated.

Figure 5 displays the mean achievable rates of macrocell UEs and femtocell UEs. In Figure 5(a) the performance is shown as the FAP intensity λ_f increases. We observe that the mean achievable rates of both macrocell and femtocell UEs only mildly decrease with the increasing of λ_f , suggesting that the network may robustly tolerate the deployment of FAPs. In Figure 5(b) the performance is shown as the outside nonsubscribers intensity λ_{out} increases. We observe that the mean achievable rates of macrocell and femtocell UEs drop initially and then tend to be stable. To interpret this behavior, we note that as the intensity of outside nonsubscribers begins to increase, more subchannels become occupied by MBSs, incurring more macrocell tier interference; however, when the intensity of outside nonsubscribers is sufficiently large, almost all the subchannels are persistently occupied by MBSs with the UEs served by time-sharing, and then the interference saturates thus leading to stable performance for UEs.

Figure 6 displays the mean achievable rates of macrocell UEs and femtocell UEs under changing transmission powers. From Figure 6(a), we observe that as the transmission power of FAPs increases, the rates of femtocell UEs increase correspondingly, and meanwhile the rates of macrocell UEs slightly decrease due to the increased cross-tier interference. The opposite trends are shown in Figure 6(b), where we observe that as the transmission power of MBSs increases, the rates of femtocell UEs deteriorate seriously, while the rates of macrocell UEs only marginally increase since they are already stuck in the interference-limited regime.

Figure 7 displays the mean achievable rates of nonsubscribers and subscribers under changing number of shared subchannels, in which the rate of nonsubscribers is averaged over both outside and inside nonsubscribers. When too few subchannels are to be shared by each FAP (i.e., small M_s), the mean achievable rate of nonsubscribers is rather low while subscribers

enjoy a good spectral efficiency. At the other extreme, when most of the subchannels are to be shared to nonsubscribers, the mean achievable rate of subscribers also deteriorates seriously. Nevertheless, from the figure we observe the existence of a stable compromise at which the rates of both subscribers and nonsubscribers do not drop much from their maxima. For the default configuration in our numerical study, the stable compromise occurs when the value of M_s lies in the range of $[7, 12]$, corresponding to a reasonably wide tuning range for system designer when provisioning the resource.

Figure 8 displays the mean achievable rate of nonsubscribers and subscribers under changing proportions of inside nonsubscribers and subscribers in femtocells. For a fair comparison, we fix the sum intensity of the two types of femtocell UEs, as $\lambda_s + \lambda_{in} = 0.03$. Figure 8(a) gives the performance in the case when most of the femtocell UEs are nonsubscribers, while Figure 8(b) corresponds to the opponent case. From the curves, we observe that in order to achieve a good performance for both types of UEs, the number of shared subchannels M_s should be adjusted based on the intensity of inside nonsubscribers.

VI. CONCLUSIONS

In this paper, we explored the application of stochastic geometry in the analysis of hybrid access mechanisms for multi-channel two-tier networks, focusing on the evaluation of the tradeoff between nonsubscribers and subscribers. We characterized several key statistics of UEs and subchannels, and established SINR distribution and mean achievable rate for each type of UEs.

Our analysis revealed the interaction among the various parameters in the network model, and thus shed useful insights into the choice of network parameters and the provisioning of resource in system design. From our numerical study, we observe that although there is an apparent conflict between the interests of nonsubscribers and subscribers, there usually exists a reasonably wide tuning range over which nonsubscribers and subscribers attain a stable compromise at which the rates of both subscribers and nonsubscribers do not drop much from their maxima.

APPENDIX A

Let r be the distance between an outside nonsubscriber and its serving MBS. Since an outside nonsubscriber always chooses its nearest MBS to access, the cdf of r is obtained by

$$\begin{aligned}\mathbb{P}\{r \leq R\} &= 1 - \mathbb{P}\{\text{no MBS closer than } R\} \\ &= 1 - e^{-\lambda_m \pi R^2}.\end{aligned}\quad (42)$$

Then, the pdf of r is given by

$$f(r) = e^{-\lambda_m \pi r^2} 2\pi \lambda_m r. \quad (43)$$

Having the pdf of r , we derive the cdf of SINR and the mean achievable rate for an outside nonsubscriber UE. Assuming that the considered UE is at distance r from its serving MBS, g is the fading of an interference link, and R is the distance between the UE and an interfering access point, the SINR experienced by the UE is given by $\text{SINR} = \frac{P_m h r^{-\alpha}}{I_c + I_f + \sigma^2}$, where $I_c = \sum_{i \in \Phi'_m \setminus \{b_0\}} P_m g_i R_i^{-\alpha}$ is the interference from the macrocell tier (excluding the serving MBS itself which is denoted by b_0) and $I_f = \sum_{j \in \Phi'_f} W P_f g_j R_j^{-\alpha}$ is the interference from the femtocell tier with the wall penetration loss taken into account.

We can thus derive the cdf of the SINR following

$$\begin{aligned}Z_m(T) &= 1 - \mathbb{P}\{\text{SINR} > T\} \\ &= 1 - \int_0^\infty 2\pi \lambda_m r e^{-\pi \lambda_m r^2} \mathbb{P}\left\{\frac{P_m h r^{-\alpha}}{I_c + I_f + \sigma^2} > T\right\} dr \\ &= 1 - \int_0^\infty 2\pi \lambda_m r e^{-\pi \lambda_m r^2} \mathbb{P}\left\{h > \frac{T r^\alpha}{P_m} (I_c + I_f + \sigma^2)\right\} dr \\ &= 1 - \int_0^\infty 2\pi \lambda_m r e^{-\pi \lambda_m r^2} \mathbb{E}\left(\exp\left(-\frac{\mu T r^\alpha}{P_m} (I_c + I_f + \sigma^2)\right)\right) dr \\ &= 1 - \int_0^\infty 2\pi \lambda_m r e^{-\pi \lambda_m r^2 - \mu T r^\alpha \sigma^2 / P_m} \mathcal{L}_{I_c + I_f}\left(\frac{\mu T r^\alpha}{P_m}\right) dr.\end{aligned}\quad (44)$$

By the definition of Laplace transform we get

$$\begin{aligned}
\mathcal{L}_{I_c+I_f}(s) &= E_{I_c+I_f}\left(e^{-s(I_c+I_f)}\right) \\
&= E_{\Phi'_m}\left(\exp\left(-s\sum_{i\in\Phi'_m\setminus\{b_0\}}P_m g_i R_i^{-\alpha}\right)\right)E_{\Phi'_f}\left(\exp\left(-s\sum_{j\in\Phi'_f}W P_f g_j R_j^{-\alpha}\right)\right) \\
&= E_{\Phi'_m}\left(\prod_{i\in\Phi'_m\setminus\{b_0\}}E_{g_i}\left(\exp\left(-s g_i R_i^{-\alpha} P_m\right)\right)\right)E_{\Phi'_f}\left(\prod_{j\in\Phi'_f}E_{g_j}\left(\exp\left(-s g_j R_j^{-\alpha} W P_f\right)\right)\right) \\
&= E_{\Phi'_m}\left(\prod_{i\in\Phi'_m\setminus\{b_0\}}\mathcal{L}_g\left(s R_i^{-\alpha} P_m\right)\right)E_{\Phi'_f}\left(\prod_{j\in\Phi'_f}\mathcal{L}_g\left(s R_j^{-\alpha} W P_f\right)\right) \\
&= \exp\left(-2\pi\lambda'_m\int_r^\infty\underbrace{\left(1-\mathcal{L}_g\left(s v^{-\alpha} P_m\right)\right)}_{(A)}v dv\right)\times \\
&\quad \exp\left(-2\pi\lambda'_f\int_0^\infty\underbrace{\left(1-\mathcal{L}_g\left(s w^{-\alpha} W P_f\right)\right)}_{(B)}w dw\right), \tag{45}
\end{aligned}$$

where the last equality follows from the pgf of PPP [15]. Next let us evaluate (A) and (B) respectively.

$$\begin{aligned}
(A) &= \int_r^\infty \int_0^\infty (1 - e^{-sv^{-\alpha}P_m g})f(g)v dg dv \\
&= \int_0^\infty \left(\int_r^\infty (1 - e^{-sv^{-\alpha}P_m g})v dv\right)f(g)dg. \tag{46}
\end{aligned}$$

Let $y = v^{-\alpha}$, then $v = y^{-\frac{1}{\alpha}}$, so we get

$$(A) = \frac{1}{\alpha} \int_0^\infty \left(\int_0^{r^{-\alpha}} (1 - e^{-sP_m g y})y^{-\frac{2}{\alpha}-1} dy\right)f(g)dg.$$

Integrating by parts, since $y^{-\frac{2}{\alpha}-1}dy = -\frac{\alpha}{2}dy^{-\frac{2}{\alpha}}$, we obtain

$$(A) = \frac{1}{\alpha} \int_0^\infty \left(\left(1 - e^{-sP_m g y}\right)y^{-\frac{2}{\alpha}}\left(-\frac{\alpha}{2}\right)\Big|_0^{r^{-\alpha}} - \int_0^{r^{-\alpha}} sP_m g e^{-sP_m g y}y^{-\frac{2}{\alpha}}\left(-\frac{\alpha}{2}\right)dy\right)f(g)dg$$

We have assumed $\alpha > 2$, so $\lim_{y \rightarrow 0}(1 - e^{-sP_m g y})y^{-\frac{2}{\alpha}} = 0$. Letting $t = sP_m g y$, we obtain

$$\begin{aligned}
(A) &= \frac{1}{2} \int_0^\infty \left(-\left(1 - e^{-sP_m g r^{-\alpha}}\right)r^2 + (sP_m g)^{\frac{2}{\alpha}} \int_0^{sP_m g r^{-\alpha}} e^{-t}t^{1-\frac{2}{\alpha}-1} dy\right)f(g)dg \\
&= -\frac{r^2}{2} + \frac{r^2}{2}\mathcal{L}_g(sP_m r^{-\alpha}) + \frac{1}{2}(sP_m)^{\frac{2}{\alpha}} \int_0^\infty g^{\frac{2}{\alpha}} \left(\Gamma\left(1 - \frac{2}{\alpha}\right) - \Gamma\left(1 - \frac{2}{\alpha}, sP_m g r^{-\alpha}\right)\right)f(g)dg.
\end{aligned}$$

From the properties of Gamma function, we have

$$\begin{aligned}\Gamma\left(1 - \frac{2}{\alpha}\right) &= -\frac{2}{\alpha}\Gamma\left(-\frac{2}{\alpha}\right) \\ \Gamma\left(1 - \frac{2}{\alpha}, sP_m gr^{-\alpha}\right) &= (sP_m gr^{-\alpha})^{-2/\alpha} e^{-sP_m gr^{-\alpha}} - \frac{2}{\alpha}\Gamma\left(-\frac{2}{\alpha}, sP_m gr^{-\alpha}\right),\end{aligned}$$

so that (A) can be simplified as

$$(A) = -\frac{r^2}{2} + \frac{1}{\alpha}(sP_m)^{\frac{2}{\alpha}}\mathbb{E}_g\left(g^{\frac{2}{\alpha}}\left(\Gamma\left(-\frac{2}{\alpha}, sP_m gr^{-\alpha}\right) - \Gamma\left(-\frac{2}{\alpha}\right)\right)\right).$$

The evaluation of (B) is almost the same, and we have

$$(B) = -\frac{1}{\alpha}(sWP_f)^{\frac{2}{\alpha}}\Gamma\left(-\frac{2}{\alpha}\right)\mathbb{E}_g\left(g^{\frac{2}{\alpha}}\right).$$

Substituting (A) and (B) into $\mathcal{L}_{I_c+I_f}(s)$ and rearranging terms in $Z_m(T)$ hence leads to (9).

Now we evaluate the mean achievable rate. Since for a positive random variable X , $\mathbb{E}[X] = \int_{t>0} \mathbb{P}\{X > t\} dt$, we have

$$\begin{aligned}\tau_m &= E[\ln(1 + \text{SINR})] \\ &= \int_0^\infty e^{-\pi\lambda_m r^2} \mathbb{E}\left[\ln\left(1 + \frac{P_m hr^{-\alpha}}{I_c + I_f + \sigma^2}\right)\right] 2\pi\lambda_m r dr \\ &= \int_0^\infty e^{-\pi\lambda_m r^2} \int_0^\infty \mathbb{P}\left\{\ln\left(1 + \frac{P_m hr^{-\alpha}}{I_c + I_f + \sigma^2}\right) > t\right\} dt 2\pi\lambda_m r dr \\ &= \int_0^\infty e^{-\pi\lambda_m r^2} \int_0^\infty \mathbb{P}\left\{h > \frac{r^\alpha}{P_m}(I_c + I_f + \sigma^2)(e^t - 1)\right\} dt 2\pi\lambda_m r dr \\ &= \int_0^\infty e^{-\pi\lambda_m r^2} \int_0^\infty \mathbb{E}\left(e^{-\mu \frac{r^\alpha}{P_m}(I_c + I_f + \sigma^2)(e^t - 1)}\right) dt 2\pi\lambda_m r dr \\ &= \int_0^\infty \int_0^\infty e^{-\pi\lambda_m r^2 - \frac{\mu r^\alpha \sigma^2}{P_m}(e^t - 1)} \mathcal{L}_{I_c+I_f}\left(\frac{\mu r^\alpha (e^t - 1)}{P_m}\right) dt 2\pi\lambda_m r dr.\end{aligned}\quad (47)$$

From the derivation of $Z_m(T)$ we have already obtained the expression of $\mathcal{L}_{I_c+I_f}\left(\frac{\mu r^\alpha (e^t - 1)}{P_m}\right)$. When substituting into (47), we arrive at (10) and thus establish Theorem 1.

APPENDIX B

Let r be the distance between a femtocell UE and its serving FAP. Because the femtocell UEs are uniformly distributed in the circular coverage area of radius R_f of each FAP, the pdf of r is given by $f(r) = 2r/R_f^2$.

Denote by I'_c and I'_f the interference strengths from the macrocell tier and the femtocell tier respectively. Similar to the proof of Theorem 1, we have

$$Z_f(T) = 1 - \int_0^{R_f} \frac{2r}{R_f^2} e^{-\frac{\mu T r^\alpha \sigma^2}{P_f}} \mathcal{L}_{I'_c+I'_f} \left(\frac{\mu T r^\alpha}{P_f} \right) dr. \quad (48)$$

Following the same procedure as in the derivation of (45), we get the Laplace transform of $I'_c + I'_f$ as

$$\begin{aligned} \mathcal{L}_{I'_c+I'_f}(s) &= E_{I'_c+I'_f} \left(e^{-s(I'_c+I'_f)} \right) \\ &= \exp \left(-2\pi\lambda'_m \int_0^\infty (1 - \mathcal{L}_g(sv^{-\alpha}WP_m))v dv - 2\pi\lambda'_f \int_0^\infty (1 - \mathcal{L}_g(sw^{-\alpha}W^2P_f))w dw \right) \\ &= \exp \left(-\pi s^{\frac{2}{\alpha}} \Gamma(1 - \frac{2}{\alpha}) (\lambda'_m (WP_m)^{\frac{2}{\alpha}} + \lambda'_f (W^2P_f)^{\frac{2}{\alpha}}) \mathbb{E}_g(g^{\frac{2}{\alpha}}) \right). \end{aligned} \quad (49)$$

In the above, it is noteworthy that the interference from an FAP penetrates two walls thus the loss becoming W^2 instead of W . Substituting (49) into (48) with $v = r^2$, we get the SINR distribution in Theorem 2. Similar to (47), the mean achievable rate is given by

$$\tau_f = \int_0^{R_f} \int_0^\infty e^{-\frac{\mu r^\alpha \sigma^2}{P_f}(e^t-1)} \mathcal{L}_{I'_c+I'_f} \left(\frac{\mu r^\alpha (e^t-1)}{P_f} \right) \frac{2r}{R_f^2} dt dr. \quad (50)$$

Substituting (49) into (50), we get the mean achievable rate in Theorem 2.

REFERENCES

- [1] G. Mansfield, "Femtocells in the US market-business drivers and consumer propositions," *FemtoCells Europe*, pp. 1927–1948, 2008.
- [2] V. Chandrasekhar, J. Andrews, and A. Gatherer, "Femtocell networks: a survey," *IEEE Communications Magazine*, vol. 46, no. 9, pp. 59–67, 2008.
- [3] H. Claussen, L. Ho, and L. Samuel, "An overview of the femtocell concept," *Bell Labs Technical Journal*, vol. 13, no. 1, pp. 221–245, 2008.
- [4] Nortel, Vodafone, "Open and closed access for home NodeBs," *3GPP, Athens, Greece, 3GPP document reference R4-071231*, 2007.
- [5] Vodafone, "Open and semi-open access support for UTRA Home NB," *3GPP-TSG RAN, Prague, Czech Republic, Tech. Rep. R2-085280*, 2008.
- [6] G. De La Roche, A. Valcarce, D. López-Pérez, and J. Zhang, "Access control mechanisms for femtocells," *IEEE Communications Magazine*, vol. 48, no. 1, pp. 33–39, 2010.
- [7] A. Valcarce, D. López-Pérez, G. De La Roche, and J. Zhang, "Limited access to OFDMA femtocells," in *Proc. IEEE 20th Int. Symp. Personal, Indoor and Mobile Radio Commun. (PIMRC)*, 2009.
- [8] M. Haenggi, J. Andrews, F. Baccelli, O. Dousse, and M. Franceschetti, "Stochastic geometry and random graphs for the analysis and design of wireless networks," *IEEE Journal on Selected Areas in Communications*, vol. 27, no. 7, pp. 1029–1046, 2009.

- [9] J. Andrews, F. Baccelli, and R. Ganti, “A tractable approach to coverage and rate in cellular networks,” *Arxiv preprint arXiv:1009.0516*, 2010.
- [10] V. Chandrasekhar and J. Andrews, “Spectrum allocation in tiered cellular networks,” *IEEE Transactions on Communications*, vol. 57, no. 10, pp. 3059–3068, 2009.
- [11] —, “Uplink capacity and interference avoidance for two-tier femtocell networks,” *IEEE Transactions on Wireless Communications*, vol. 8, no. 7, pp. 3498–3509, 2009.
- [12] P. Xia, V. Chandrasekhar, and J. Andrews, “Open vs. closed access femtocells in the uplink,” *IEEE Transactions on Wireless Communications*, vol. 9, no. 12, pp. 3798–3809, 2010.
- [13] H. Jo, P. Xia, and J. Andrews, “Open, closed, and shared access femtocells in the downlink,” *Arxiv preprint arXiv:1009.3522*, 2010.
- [14] J. Ferenc and Z. Nédá, “On the size distribution of Poisson Voronoi cells,” *Physica A: Statistical Mechanics and its Applications*, vol. 385, no. 2, pp. 518–526, 2007.
- [15] D. Stoyan, W. Kendall, J. Mecke, and D. Kendall, *Stochastic Geometry and Its Applications*, Wiley, New York, 1995.

TABLE I
SYSTEM PARAMETERS

Symbol	Description	Value
Φ_m, Φ_f	PPPs defining the MBSs and FAPs	N/A
λ_m	Density of MBSs	0.00001 MBS/m ²
λ_f	Density of FAPs	0.0001 FAP/m ²
R_f	Radius of femtocell	10m
λ_{out}	Densities of outside nonsubscribers	0.0001 user/m ²
λ_s, λ_{in}	Densities of subscribers and inside nonsubscribers	0.015 user/m ²
P_m, P_f	Transmit power at MBS and FAP	39dBm, 13dBm
M	Number of subchannels at each access point	20
M_s, M_r	Number of subchannels shared and reserved by each femtocell	Not fixed
α	Path loss exponent	4
μ	Rayleigh fading parameter	1 (normalized)
W	Wall penetration loss	-6dB
σ^2	Noise power	0 (interference-limited regime)
P_{busy}^m, P_{busy}^f	Probabilities that a given subchannel is used by an MBS and an FAP	Not fixed
Φ'_m, Φ'_f	PPPs defining the MBSs and FAPs that interfere a given subchannel	N/A
λ'_m, λ'_f	Densities of MBSs and FAPs that interfere a given subchannel	Not fixed
U_{out}, U_{in}	Numbers of nonsubscribers that access a given MBS and a given FAP	Not fixed
U_s	Numbers of subscribers that access a given FAP	Not fixed
τ_f, τ_m	Mean achievable rates of femtocell UEs and macrocell UEs	Not fixed
τ_s, τ_n	Mean achievable rates of subscribers and nonsubscribers	Not fixed

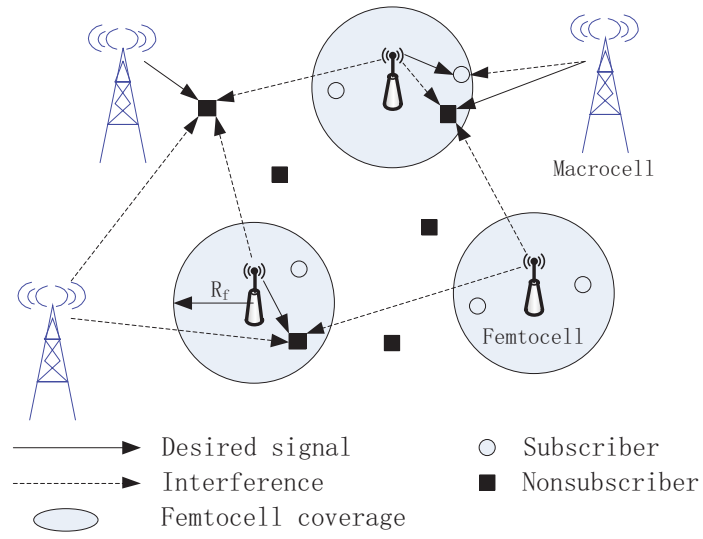


Fig. 1. Downlink two-tier network model for hybrid access femtocell.

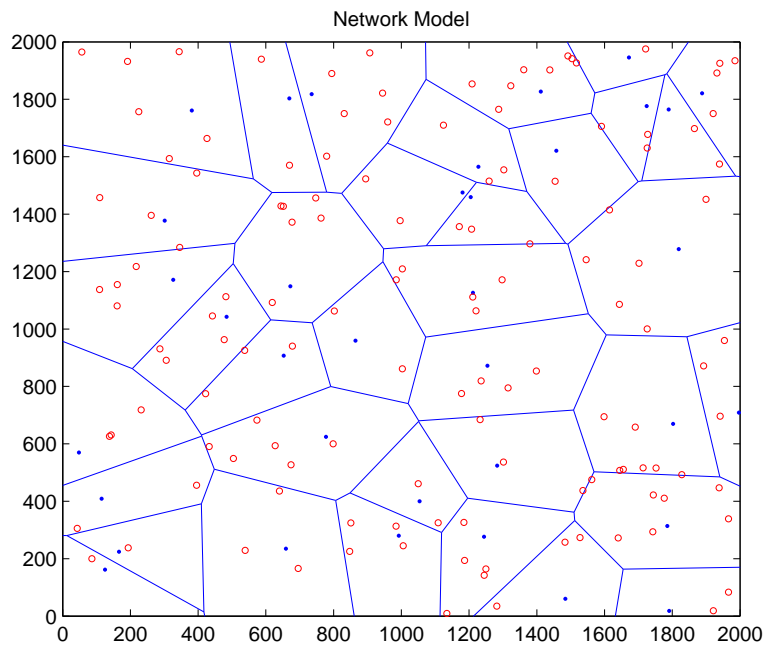


Fig. 2. The Voronoi macrocell topology, in which each Voronoi cell is the coverage area of a macrocell and each small circle represents a femtocell coverage area.

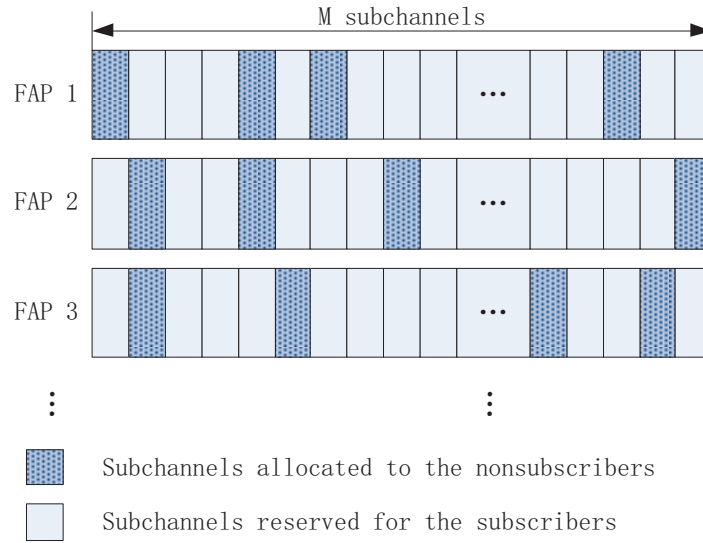


Fig. 3. Spectrum allocation in each hybrid access femtocell. All the M_s shared subchannels are randomly selected by each FAP.

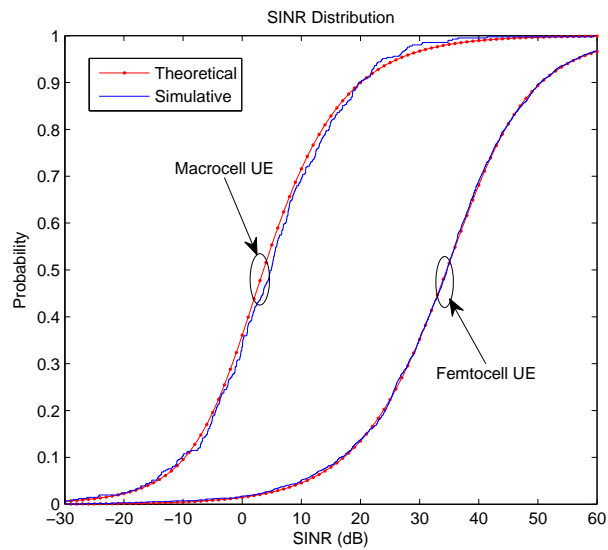


Fig. 4. Cdfs of SINRs for macrocell UEs and femtocell UEs, when $M_s = 10$.

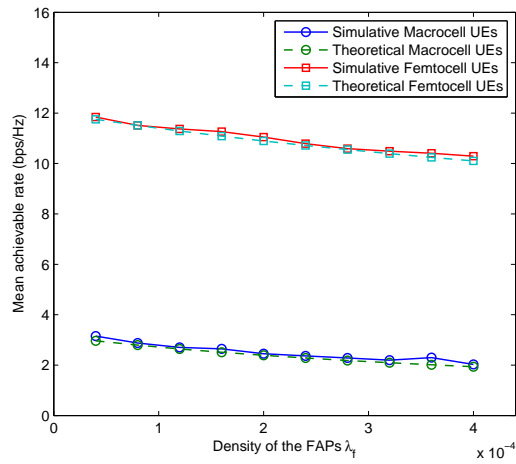
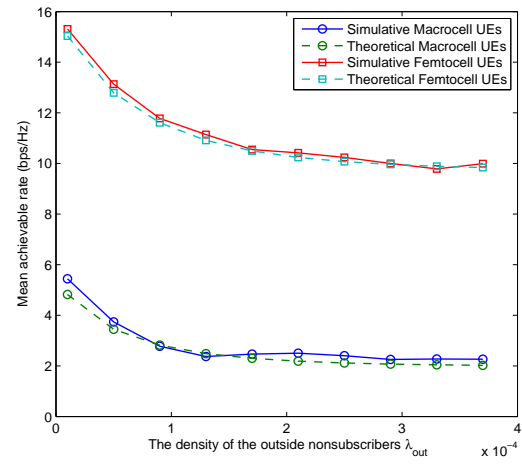
(a) Change the intensity of FAPs λ_f .(b) Change the intensity of outside nonsubscribers λ_{out} .

Fig. 5. Mean achievable rates of macrocell UEs and femtocell UEs with changing intensities of FAPs and outside nonsubscribers.

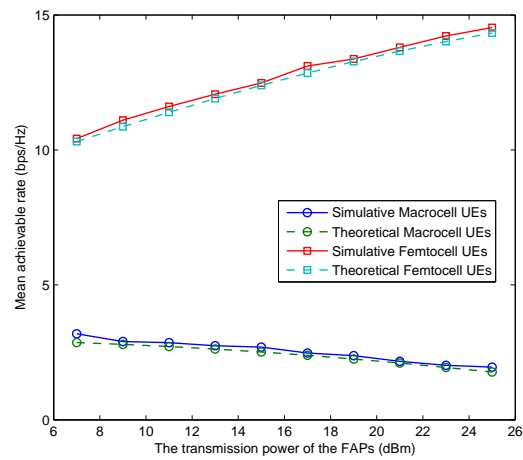
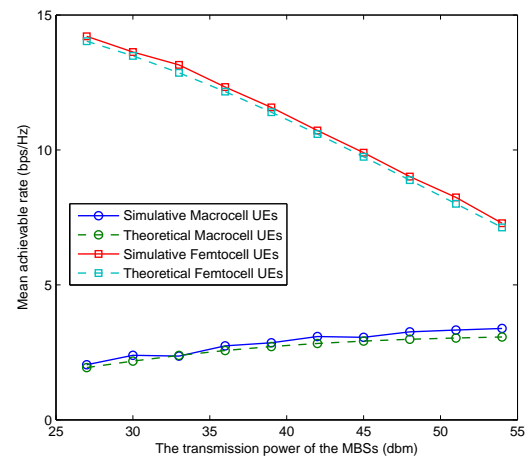
(a) Change P_f , $P_m = 39\text{dBm}$ fixed.(b) Change P_m , $P_f = 13\text{dBm}$ fixed.

Fig. 6. Mean achievable rates of macrocell UEs and femtocell UEs with changing transmission powers.

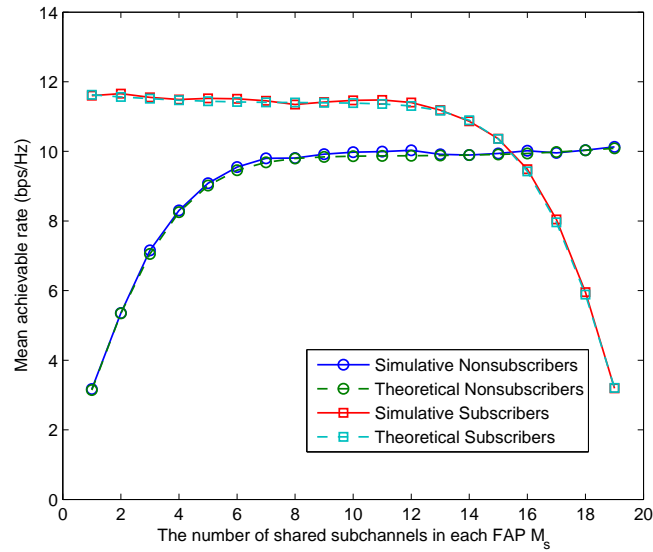
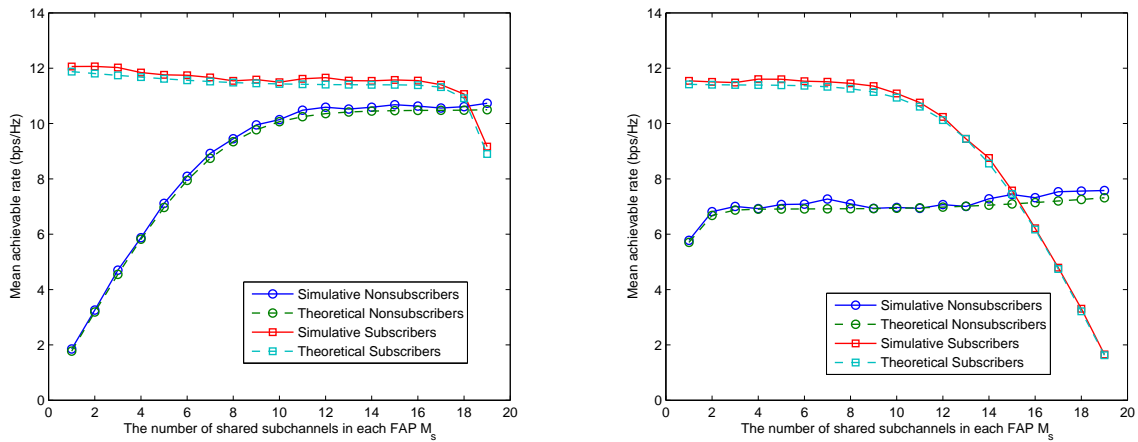


Fig. 7. Performance of nonsubscribers and subscribers with changing number of shared subchannels M_s .



(a) $\lambda_s = 0.003$ and $\lambda_{in} = 0.027$.

(b) $\lambda_s = 0.027$ and $\lambda_{in} = 0.003$.

Fig. 8. Performance of nonsubscribers and subscribers with changing proportions of inside nonsubscribers and subscribers.

Multi-channel Hybrid Access Femtocells: A Stochastic Geometric Analysis

Yi Zhong and Wenyi Zhang, *Senior Member, IEEE*

Abstract

[TO UPDATE] For femtocells, the channel access mechanism can be configured to be open access or closed access. Open access may lead to performance deterioration for femtocell subscribers, while closed access may cause serious interference to nonsubscribers served by macrocells. A compromise solution is hybrid access, in which only a fraction of the available resource is shared to nonsubscribers while the remaining reserved for subscribers. This paper focuses on a hybrid access mechanism for multi-channel femtocells which employ orthogonal spectrum access schemes, like OFDMA. Considering a randomized channel assignment strategy, we analyze the performance in the downlink. Using stochastic geometry as technical tools, we derive the blocking probabilities, mean achievable rates, and distributions of the signal-to-interference-plus-noise ratio of both nonsubscribers and subscribers. For these key performance indicators, we establish either explicit or integral closed form expressions, which are amenable to numerical evaluations. The analysis reveals the performance tradeoff between subscribers and nonsubscribers, and is corroborated by numerical simulations.

Index Terms

Channel management, femtocell, hybrid access, spatial Poisson process, two-scale approximation, two-tier network

The authors are with Department of Electronic Engineering and Information Science, University of Science and Technology of China, Hefei 230027, China (email: geners@mail.ustc.edu.cn, wenyizha@ustc.edu.cn). The research has been supported by MIIT of China through grant 2011ZX03001-006-01 and by the Doctorial Program of Higher Education of China through grant 20103402120023.

I. INTRODUCTION

In current cellular network services, about 50% of phone calls and 70% of data services take place indoors [?]. For such indoor use cases, network coverage is a critical issue. One way to improve the indoor performance is to deploy the so-called femtocell access points (FAPs), also known as home base stations, besides macrocell base stations (MBSs). Femtocells are small cellular base stations, typically designed for use in home or small business [?][?]. The use of femtocells not only benefits the users, but also the operators. As the distance between the transmitter and receiver is reduced, users will enjoy high quality links and power savings. Furthermore, the reduced transmission range also creates more spatial reuse and reduces electromagnetic interference.

Among the many challenges faced by femtocells, and more generally, two-tier networks, is the issue of interference; see Figure 1. The two-tier interference problem differs from that in traditional single-tier networks in several important aspects: First, due to the limitations of access mechanism, a user equipment (UE) may not be able to connect to the access point which offers the best service. Second, since femtocells connect to operator's core network via subscribers' private ISP, coordination between macrocells and femtocells and among femtocells is limited. Finally, compared to planned macrocell deployments, femtocells are usually deployed in an ad hoc manner, and the thus randomly placed femtocells make it difficult to manage the interference. In two-tier networks comprising of macrocells and femtocells, interference can be categorized into two types:

- **Cross-tier:** This refers to the interference from one tier to the other; that is, femtocell interference at a macrocell and macrocell interference at a femtocell.
- **Co-tier:** This refers to the interference within a tier; that is, femtocell interference at a nearby femtocell and macrocell interference at a nearby macrocell.

In this paper, we consider two-tier networks that are based on multicarrier techniques, for example those deploying LTE or WiMAX standards, which use orthogonal frequency-division multiple access (OFDMA) techniques. In multicarrier systems, the available spectrum is divided into orthogonal subcarriers, which are then grouped into multiple subchannels, assigned to different users. Due to the flexibility in channel assignment, both cross-tier and co-tier interferences may be alleviated.

The access mechanism of femtocells (see, e.g., [?]) is a key factor that affects the performance of two-tier networks, and generally can be classified as follows, where we call the UEs that register to a femtocell as subscribers, and those that do not register to any femtocell as nonsubscribers.

- **Closed access:** An FAP only allows its subscribers to connect.
- **Open access:** An FAP allows all its covered UEs, no matter registered or not, to connect.
- **Hybrid access:** An FAP allows its covered nonsubscribers to connect via a subset of its available subchannels, and reserves the remaining subchannels for its subscribers.

Hybrid access [?] is an intermediate approach, in which a fraction of the total available resource is allocated to nonsubscribers. By doing so, nonsubscribers near an FAP may handover into the femtocell to avoid high interference; meanwhile, with a certain amount of resource reserved for subscribers, the performance of subscribers may be well assured even in the presence of nonsubscribers.

In hybrid access, a central issue is how to allocate the resource between subscribers and nonsubscribers. Previous studies [?] [?] indicate that hybrid access improves the network performance at the cost of reduced performance for subscribers, therefore suggesting a tradeoff between the performance of nonsubscribers and subscribers. In this paper, we consider a hybrid access mechanism that uses a randomized channel assignment strategy, and analyze the performance in the downlink of both macrocells and femtocells. We employ stochastic geometry to characterize the spatial distributions of users as well as access points; see, e.g., [?] and references therein for its recent applications in wireless networks. Accordingly, we derive the key performance indicators including blocking probabilities, mean achievable rates, and distributions of the signal-to-interference-plus-noise ratios (SINRs), of both nonsubscribers and subscribers. In our study, we establish general integral expressions for the performance indicators, and closed form expressions under specific model parameters. With the obtained results, we reveal how the performance of subscribers and nonsubscribers trades off each other.

An overview of related works is as follows. In [?], the authors proposed to study key performance indicators for cellular networks, such as coverage probabilities and mean achievable rates, through models and tools in stochastic geometry. Our work explores that approach in hybrid access femtocell networks, focusing on multi-channel models and the downlink performance. In [?], the considered scheme divides the spectrum resource into two orthogonal parts which are

assigned to macrocells and femtocells, respectively, with femtocells being closed access. In [?], the authors considered two-tier femtocell networks using time-hopped CDMA, examining the uplink outage probability and the interference avoidance capability. In [?] and [?], the authors studied the performance of various femtocell access mechanisms, under substantially different system models from ours. Our work examines the interaction among multiple MBSs and FAPs, and focuses on scenarios in which macrocells and femtocells share the same frequency band, following a hybrid access mechanism, as will be elaborated in Section II.

The remaining part of the paper is organized as follows. Section II describes the two-tier network model, the channel assignment strategy, and the hybrid access mechanism. Based on a two-scale approximation for the spatial distributions of femtocells, Section III analyzes the statistical behavior of UEs, deriving the distributions of the number of UEs connecting to either an FAP or an MBS, as well as the probabilities of a subchannel being used by either an FAP or an MBS. Built upon those statistics, Section IV establishes expressions for the distributions of the SINRs, and the mean achievable rates. Section V illustrates the aforementioned analysis by numerical results, which are also corroborated by simulations. Finally, Section VI concludes the paper.

II. NETWORK MODEL

A. Hybrid Access Femtocells

In the two-tier network, we consider two types of access points, MBSs and FAPs. The MBSs constitute the macrocell tier, and they induce a Voronoi tessellation of the plane (see Figure 2). When a UE attempts to access the macrocell network, it chooses to connect to the MBS in the Voronoi cell which it is situated in. An FAP provides network access to UEs in its vicinity, and we assume that all FAPs have a covering radius of R_f . Within the covered circular area of each FAP are two types of UEs, called subscribers and inside nonsubscribers. Inside nonsubscribers are those UEs who gather around an FAP without subscribing to its service; for example, transient customers in a shop or restaurant. Besides those two types of UEs, we also consider a third type of UEs, outside nonsubscribers, who are uniformly scattered over the whole plane, corresponding to those regular macrocell network users.

The available spectrum is evenly divided into M subchannels, which are to be shared by both the macrocell tier and the femtocell tier. Each FAP is configured to allocate a fixed number, M_s ,

of subchannels for its covered inside nonsubscribers. These M_s subchannels are called shared subchannels, and the remaining $M_r = M - M_s$ subchannels are called reserved subchannels as they are reserved for the subscribers. In the considered hybrid access mechanism, each FAP selects its shared subchannels randomly, and independently of other FAPs. We assume that each UE, whether subscriber or nonsubscriber, needs one subchannel for accessing the two-tier network. When a UE accessing an MBS or an FAP, the serving subchannel is selected randomly (see Figure 3).

The hybrid access mechanism operates as follows.

- A subscriber accesses to one of the M_r reserved subchannels of its corresponding FAP. When there are more than M_r subscribers in an FAP, they are served by time-sharing with equal time proportion.
- An inside nonsubscriber accesses to one of the M_s shared subchannels of its covering FAP. When there are more than M_s inside nonsubscribers in an FAP, they are served by time-sharing with equal time proportion.
- An outside nonsubscriber accesses the MBS in the Voronoi cell which the outside nonsubscriber is situated in. When there are more than M outside nonsubscribers in the Voronoi cell, they are served by time-sharing with equal proportion.

B. Mathematical Model and Two-scale Approximation

To formulate the aforementioned hybrid access scenario mathematically, we model the spatial distributions of the nodes using spatial Poisson processes as follows. The MBSs constitute a homogeneous Poisson point process (PPP) Φ_m of intensity λ_m on the plane; the FAPs constitute another homogeneous PPP Φ_f of intensity λ_f . In the circular covered area of radius R_f of each FAP, the subscribers are distributed according to a homogeneous PPP of intensity λ_s , and the inside nonsubscribers are distributed according to another homogeneous PPP of intensity λ_{in} . Outside nonsubscribers constitute on the whole plane a homogeneous PPP of intensity λ_{out} . All the PPPs are mutually independent.

In this paper, we focus on the downlink performance. The transmit power is set to a constant value P_m for an MBS, and P_f for an FAP. For the sake of convenience, we adopt a standard path loss propagation model with path loss exponent $\alpha > 2$. Regarding fading, we assume that the link between the serving access point (either an MBS or an FAP) and the served UE experiences

Rayleigh fading with parameter μ . The received signal power of a UE at a distance r from its serving access point therefore is $P_m hr^{-\alpha}$ (MBS) or $P_f hr^{-\alpha}$ (FAP) where $h \sim \text{Exp}(\mu)$. The fading of interference links may follow an arbitrary probability distribution, and is denoted by g . Furthermore, considering the typical scenario of indoor femtocell deployment, we introduce a wall isolation at the boundary of each FAP coverage area, which incurs a wall penetration loss factor $W < 1$. For all receivers, the noise power is σ^2 .

The different PPPs corresponding to different entities in the network interact in a complicated way, thus making a rigorous statistical analysis extremely difficult. For example, an inside nonsubscriber may be covered by more than one FAPs, thus leading to the delicate issue of FAP selection, and furthermore rendering the subchannel usage distributions among FAPs and MBSs intrinsically correlated. To overcome the technical difficulties due to spatial interactions, in the subsequent analysis we propose a two-scale approximation for the network model, motivated by the fact that the covered area of an FAP is significantly smaller than that of an MBS. The two-scale approximation consists of two views, the macro-scale view and the micro-scale view. The macro-scale view concerns an observer outside the coverage area of an FAP, and in that view the whole coverage area of the FAP shrinks to a single point, marked by the numbers of subscribers and inside nonsubscribers therein. The micro-scale view concerns an observer inside the coverage area of an FAP, and in that view the coverage area is still circular with radius R_f in which the subscribers and inside nonsubscribers are spatially distributed. By such a two-scale approximation, an inside nonsubscriber can only be covered by a unique FAP, and the coverage area of an FAP can only be within a unique Voronoi cell of an MBS. These consequences substantially simplify the performance analysis. In Section V, we validate the two-scale approximation method through comparing analytical results and simulation results, for network parameters of practical interest.

III. STATISTICS OF UES AND SUBCHANNELS

In this section, we characterize the distributions of UEs connecting to different types of access points, and the distributions of used subchannels in MBSs and FAPs. The analysis is based on a snapshot of the network model, and the obtained results will then be applied for characterizing the distributions of SINRs and achievable rates in Section IV.

A. Distributions of UEs

Let U_s be the number of subscribers accessing a given FAP and from our model we have $U_s \sim \text{Poisson}(\lambda_s \pi R_f^2)$. Similarly, let U_{in} be the number of inside nonsubscribers accessing a given FAP, and we have $U_{\text{in}} \sim \text{Poisson}(\lambda_{\text{in}} \pi R_f^2)$.

The number of outside nonsubscribers who access a given MBS, denoted by U_{out} , is characterized as follows. We note that the macrocell coverage area is a Voronoi cell, and denote by S the area of the Voronoi cell. There is no known closed form expression of the probability density function (pdf) of S , whereas a simple approximation [?] has proven sufficiently accurate for practical purposes. Considering scaling, the approximate pdf of the size of a macrocell coverage area is given by

$$f(S) = \frac{343}{15} \sqrt{\frac{7}{2\pi}} (S\lambda_m)^{\frac{5}{2}} \exp\left(-\frac{7}{2}S\lambda_m\right)\lambda_m. \quad (1)$$

Conditioned upon S , the number of outside nonsubscribers is a Poisson random variable with mean $\lambda_{\text{out}}S$. The probability generating function (pgf) of the unconditioned U_{out} is thus given by

$$G(z) = \int_0^\infty \exp\left(\lambda_{\text{out}}(z-1)S\right) f(S) dS. \quad (2)$$

Plugging in the approximate pdf of S and simplifying the integral, we get

$$G(z) = \frac{343}{8} \sqrt{\frac{7}{2}} \left(\frac{7}{2} - \frac{\lambda_{\text{out}}}{\lambda_m}(z-1)\right)^{-\frac{7}{2}}. \quad (3)$$

The distribution of U_{out} is therefore given by the derivatives of $G(z)$,

$$\mathbb{P}\{U_{\text{out}} = i\} = \frac{G^{(i)}(0)}{i!}, \quad i = 0, 1, \dots \quad (4)$$

B. Distributions of Subchannel Usage

Since the subchannels are uniformly and independently selected by each FAP, it suffices to analyze an arbitrary one of them. Let us examine the probability that a given subchannel is used by an MBS or an FAP. In order to obtain the probability, we evaluate the average number of subchannels used by an MBS or an FAP, and then normalize the average number by the total number of subchannels, M .

The probability that a subchannel is used by an FAP is

$$\begin{aligned}
P_{\text{busy},f} &= \frac{1}{M} \left(\sum_{i=0}^{\infty} \min\{i, M_r\} \mathbb{P}\{U_s = i\} + \sum_{j=0}^{\infty} \min\{j, M_s\} \mathbb{P}\{U_{\text{in}} = j\} \right) \\
&= \frac{1}{M} \sum_{i=0}^{M_r} i \mathbb{P}\{U_s = i\} + \left(1 - \frac{M_s}{M}\right) \sum_{i=M_r+1}^{\infty} \mathbb{P}\{U_s = i\} + \\
&\quad + \frac{1}{M} \sum_{j=0}^{M_s} j \mathbb{P}\{U_{\text{in}} = j\} + \frac{M_s}{M} \sum_{j=M_s+1}^{\infty} \mathbb{P}\{U_{\text{in}} = j\}. \tag{5}
\end{aligned}$$

For a Poisson random variable $N \sim \text{Poisson}(\lambda)$, its cumulative distribution function (cdf) is given by

$$\sum_{i=0}^n \mathbb{P}\{N = i\} = \sum_{i=0}^n \frac{\lambda^i}{i!} e^{-\lambda} = \frac{\Gamma(n+1, \lambda)}{n!}, \tag{6}$$

where $\Gamma(s, x) = \int_x^{\infty} t^{s-1} e^{-t} dt$ is the incomplete gamma function. Using (6) to simplify $P_{\text{busy},f}$, we get

$$\begin{aligned}
P_{\text{busy},f} &= 1 + \frac{M_r}{M} \frac{1}{M_r!} \left(\lambda_s \pi R_f^2 \Gamma(M_r, \lambda_s \pi R_f^2) - \Gamma(M_r + 1, \lambda_s \pi R_f^2) \right) + \\
&\quad + \frac{M_s}{M} \frac{1}{M_s!} \left(\lambda_{\text{in}} \pi R_f^2 \Gamma(M_s, \lambda_{\text{in}} \pi R_f^2) - \Gamma(M_s + 1, \lambda_{\text{in}} \pi R_f^2) \right). \tag{7}
\end{aligned}$$

The probability that a subchannel is used by an MBS is

$$P_{\text{busy},m} = \frac{1}{M} \sum_{i=0}^{\infty} \min\{i, M\} \mathbb{P}\{U_{\text{out}} = i\}, \tag{8}$$

where $\mathbb{P}\{U_{\text{out}} = i\}$ is given by (4).

The spatial process of FAPs that use a given subchannel is the independent thinning of the original PPP of FAPs Φ_f by the probability $P_{\text{busy},f}$, denoted by Φ'_f with intensity $\lambda'_f = \lambda_f P_{\text{busy},f}$. The term ‘‘independent thinning’’ means that Φ'_f can be viewed as obtained from Φ_f by independently removing points with probability $1 - P_{\text{busy},f}$. Similarly, the spatial process of MBSs that use a given subchannel is the independent thinning of the original PPP of MBSs Φ_m by the probability $P_{\text{busy},m}$, denoted by Φ'_m with intensity $\lambda'_m = \lambda_m P_{\text{busy},m}$. These two independently thinned PPPs will prove useful in the subsequent analysis.

IV. ANALYSIS OF SINR AND MEAN ACHIEVABLE RATE

In this section, we derive the distributions of SINRs and the mean achievable rates of all the three types of UEs. For each type of UEs, we begin with general settings, and then simplify the

general results under several specific parameters to gain insights. The mean achievable rates are the averaged instantaneous achievable rates over both channel fading and spatial distributions of UEs and access points.

A. Macrocell UEs

1) *General Case:* For an active UE served by an MBS, it must be occupying one subchannel of the MBS. The following theorem gives the cdf of SINR and the mean achievable rate of each active macrocell UE in general case.

Theorem 1: The cdf of the SINR of a macrocell UE, denoted by $Z_m(T) = \mathbb{P}\{\text{SINR} \leq T\}$, is given by

$$Z_m(T) = 1 - \pi \lambda_m \int_0^\infty \exp\left(\pi v \lambda'_m \left(1 - \beta(T, \alpha) - \frac{1}{P_{\text{busy},m}}\right) - \frac{\mu T v^{\frac{\alpha}{2}} \sigma^2}{P_m}\right) dv. \quad (9)$$

The mean achievable rate of a macrocell UE is given by

$$\tau_m = \pi \lambda_m \int_0^\infty \int_0^\infty \exp\left(\pi v \lambda'_m \left(1 - \beta(e^t - 1, \alpha) - \frac{1}{P_{\text{busy},m}}\right) - \frac{\mu v^{\frac{\alpha}{2}} \sigma^2 (e^t - 1)}{P_m}\right) dt dv. \quad (10)$$

In (9) and (10), $\beta(T, \alpha)$ is given by

$$\beta(T, \alpha) = \frac{2(\mu T)^\frac{2}{\alpha}}{\alpha} \mathbb{E}_g \left(g^\frac{2}{\alpha} \left(\Gamma\left(-\frac{2}{\alpha}, \mu T g\right) - \left(1 + \frac{\lambda'_f (W P_f)^\frac{2}{\alpha}}{\lambda'_m P_m^\frac{2}{\alpha}}\right) \Gamma\left(-\frac{2}{\alpha}\right) \right) \right). \quad (11)$$

The proof of Theorem 1 is in Appendix A.

In Theorem 1, $Z_m(T)$ in (9) gives the probability that the SINR is below a given target level T , and τ_m in (10) gives the mean achievable rate of a macrocell UE. The integrals in (9) and (10) can be evaluated by numerical methods, and furthermore, they can be simplified to concise forms in a number of special cases. The cases of interest in this paper are the combinations of (i) interference experiencing Rayleigh fading, (ii) the path loss exponent being $\alpha = 4$, and (iii) no noise or the noise is weak, $\sigma^2 \rightarrow 0$. The following discussions are categorized into two parts according to the interference fading.

2) *Special Case When Interference Experiences General Fading:*

a) *General Fading, Noise, $\alpha = 4$:* We can simplify (9) via invoking the identity

$$\int_0^\infty e^{-ax} e^{-bx^2} dx = \sqrt{\frac{\pi}{b}} \exp\left(\frac{a^2}{4b}\right) Q\left(\frac{a}{\sqrt{2b}}\right), \quad (12)$$

where $Q(x) = \frac{1}{\sqrt{2\pi}} \int_x^\infty \exp(-y^2/2) dy$ is the standard Gaussian tail probability. Letting $a(T) = \pi\lambda'_m(\beta(T, 4) + \lambda_m/\lambda'_m - 1)$, we have

$$Z_m(T) = 1 - \pi\lambda_m \sqrt{\frac{\pi P_m}{\mu T \sigma^2}} \exp\left(\frac{a^2(T) P_m}{4\mu T \sigma^2}\right) Q\left(a(T) \sqrt{\frac{P_m}{2\mu T \sigma^2}}\right). \quad (13)$$

For a given distribution of interference fading, $\beta(T, 4)$ can be evaluated by numeric methods, and subsequently the SINR distribution $Z_m(T)$ can be obtained conveniently.

b) General Fading, Small Noise, $\alpha > 2$: Consider the interference-limited regime in which the noise power is approaching zero. Using the expansion $e^{-x} = 1 - x + o(x)$ as $x \rightarrow 0$, the SINR distribution behaves like

$$Z_m(T) = 1 - \frac{1}{1 + (\beta(T, \alpha) - 1) P_{\text{busy},m}} + \frac{\pi\lambda_m \mu T \sigma^2 \Gamma(\alpha/2 + 1)}{\left(\pi\lambda'_m (\beta(T, \alpha) + \lambda_m/\lambda'_m - 1)\right)^{\alpha/2+1} P_m} + o(\sigma^2). \quad (14)$$

When $\sigma^2 = 0$, the SINR distribution is further simplified into

$$Z_m(T) = 1 - \frac{1}{1 + (\beta(T, \alpha) - 1) P_{\text{busy},m}}. \quad (15)$$

3) Special Case When Interference Experiences Rayleigh Fading: Here we consider the case where the interference experiences Rayleigh fading with mean μ , i.e. $g \sim \text{Exp}(\mu)$. In this case, the results are simplified as follows.

Corollary 1: When the interference follows Rayleigh fading, the cdf of the SINR is

$$Z_m(T) = 1 - \pi\lambda_m \int_0^\infty \exp\left(-\pi v \lambda_m - \pi v \lambda'_m \varphi(T, \alpha, T^{-2/\alpha}) - \pi v \lambda'_f \varphi\left(\frac{P_f W T}{P_m}, \alpha, 0\right) - \frac{\mu T v^{\alpha/2} \sigma^2}{P_m}\right) dv. \quad (16)$$

The mean achievable rate is

$$\tau_m = \pi\lambda_m \int_0^\infty \int_0^\infty \exp\left(-\pi v \lambda_m - \pi v \lambda'_m \varphi\left(e^t - 1, \alpha, (e^t - 1)^{-2/\alpha}\right) - \pi v \lambda'_f \varphi\left(\frac{P_f W (e^t - 1)}{P_m}, \alpha, 0\right) - \frac{\mu v^{\alpha/2} \sigma^2 (e^t - 1)}{P_m}\right) dv dt, \quad (17)$$

where

$$\varphi(T, \alpha, x) = T^{2/\alpha} \int_x^\infty \frac{1}{1 + u^{\alpha/2}} du. \quad (18)$$

The results in Corollary 1 are further simplified in the following special cases.

a) *Rayleigh Fading, Noise*, $\alpha = 4$: Using (12), we get

$$Z_m(T) = 1 - \pi\lambda_m \sqrt{\frac{\pi P_m}{\mu T \sigma^2}} \exp\left(\frac{\kappa^2(T) P_m}{4\mu T \sigma^2}\right) Q\left(\kappa(T) \sqrt{\frac{P_m}{2\mu T \sigma^2}}\right). \quad (19)$$

The mean achievable rate of a macrocell UE is simplified into

$$\tau_m = \pi\lambda_m \int_0^\infty \sqrt{\frac{\pi P_m}{\mu \sigma^2 (e^t - 1)}} \exp\left(\frac{\kappa^2(e^t - 1) P_m}{4\mu \sigma^2 (e^t - 1)}\right) Q\left(\kappa(e^t - 1) \sqrt{\frac{P_m}{2\mu \sigma^2 (e^t - 1)}}\right) dt, \quad (20)$$

where

$$\kappa(T) = \pi\lambda_m + \pi\lambda'_m \sqrt{T} (\pi/2 - \arctan \sqrt{T}) + \frac{\pi^2 \lambda'_f}{2} \sqrt{\frac{P_f W T}{P_m}}. \quad (21)$$

b) *Rayleigh Fading, No Noise*, $\alpha > 2$: When $\sigma^2 = 0$, the SINR distribution is simplified into

$$Z_m(T) = 1 - \frac{1}{1 + \frac{\lambda'_m}{\lambda_m} \varphi(T, \alpha, T^{-2/\alpha}) + \frac{\lambda'_f}{\lambda_m} \varphi\left(\frac{P_f W T}{P_m}, \alpha, 0\right)}. \quad (22)$$

The mean achievable rate of a macrocell UE is simplified into

$$\tau_m = \int_0^\infty \frac{1}{1 + \frac{\lambda'_m}{\lambda_m} \varphi(e^t - 1, \alpha, (e^t - 1)^{-2/\alpha}) + \frac{\lambda'_f}{\lambda_m} \varphi\left(\frac{P_f W (e^t - 1)}{P_m}, \alpha, 0\right)} dt. \quad (23)$$

Specifically, when $\alpha = 4$ we obtain

$$Z_m(T) = 1 - \frac{1}{1 + \sqrt{T} \left(\frac{\pi}{2} - \arctan \sqrt{T} + \frac{\pi}{2} \frac{\lambda'_f}{\lambda'_m} \sqrt{\frac{W P_f}{P_m}} \right) P_{\text{busy},m}}. \quad (24)$$

The mean achievable rate of a macrocell UE is simplified into

$$\tau_m = \int_0^{\pi/2} \frac{2}{\tan y + (\pi/2 - y) P_{\text{busy},m} + \frac{\pi}{2} \frac{\lambda'_f}{\lambda'_m} \sqrt{\frac{W P_f}{P_m}}} dy. \quad (25)$$

From a practical perspective, it is desirable to shape $Z_m(T)$ to make it small for small values of T . From (24), we see that there are two approaches to shape $Z_m(T)$. First, $Z_m(T)$ decreases as $P_{\text{busy},m}$, the probability that a subchannel is used by an MBS, decreases. This may be interpreted as an effect of frequency reuse. Second, $Z_m(T)$ decreases as the whole term, $\frac{\lambda'_f}{\lambda'_m} \sqrt{\frac{W P_f}{P_m}}$, decreases, which corresponds to a number of network parameters, representing the effect due to the deployment of the femtocell tier.

B. Femtocell UEs

1) *General Case*: A UE served by an FAP occupies one subchannel of the FAP. The following theorem gives the cdf of SINR and the mean achievable rate of each active femtocell UE in general case.

Theorem 2: The cdf of the SINR of a femtocell UE in general case is given by

$$Z_f(T) = 1 - \frac{1}{R_f^2} \int_0^{R_f^2} \exp\left(-\rho(\alpha)T^{2/\alpha}v - \frac{\mu T v^{\alpha/2} \sigma^2}{P_f}\right) dv. \quad (26)$$

The mean achievable rate of a femtocell UE is given by

$$\tau_f = \frac{1}{R_f^2} \int_0^{R_f^2} \int_0^\infty \exp\left(-\rho(\alpha)(e^t - 1)^{2/\alpha}v - \frac{\mu v^{\alpha/2} \sigma^2 (e^t - 1)}{P_f}\right) dt dv. \quad (27)$$

in (26) and (27), $\rho(\alpha)$ is given by

$$\rho(\alpha) = -\frac{2\pi\mu^{2/\alpha}}{\alpha} \Gamma\left(-\frac{2}{\alpha}\right) \left(\lambda'_m \left(\frac{WP_m}{P_f}\right)^{2/\alpha} + \lambda'_f W^{4/\alpha}\right) \mathbb{E}_g(g^{2/\alpha}). \quad (28)$$

The proof of Theorem 2 is in Appendix B.

2) Special Case When Interference Experiences General Fading:

a) *General Fading, Noise, $\alpha = 4$* : Using the following identity to simplify the results in Theorem 2,

$$\int_0^u e^{-ax} e^{-bx^2} dx = \sqrt{\frac{\pi}{b}} \exp\left(\frac{a^2}{4b}\right) \left(\text{Q}\left(\frac{a}{\sqrt{2b}}\right) - \text{Q}\left(\frac{a}{\sqrt{2b}} - u\sqrt{b}\right)\right), \quad (29)$$

we get the SINR distribution as

$$Z_f(T) = 1 - \frac{1}{R_f^2} \sqrt{\frac{\pi P_f}{\mu T \sigma^2}} \exp\left(\frac{\rho^2(4)P_f}{4\mu\sigma^2}\right) \left(\text{Q}\left(\rho(4)\sqrt{\frac{P_f}{2\mu\sigma^2}}\right) - \text{Q}\left(\rho(4)\sqrt{\frac{P_f}{2\mu\sigma^2}} - R_f^2 \sqrt{\frac{\mu\sigma^2 T}{P_f}}\right)\right). \quad (30)$$

The mean achievable rate is simplified into

$$\tau_f = \frac{1}{R_f^2} \sqrt{\frac{\pi P_f}{\mu\sigma^2}} \exp\left(\frac{\rho^2(4)P_f}{4\mu\sigma^2}\right) \int_0^\infty \psi(t) dt, \quad (31)$$

where

$$\psi(t) = \frac{1}{\sqrt{e^t - 1}} \left(\text{Q}\left(\rho(4)\sqrt{\frac{P_f}{2\mu\sigma^2}}\right) - \text{Q}\left(\rho(4)\sqrt{\frac{P_f}{2\mu\sigma^2}} - R_f^2 \sqrt{\frac{\mu\sigma^2(e^t - 1)}{P_f}}\right)\right).$$

b) *General Fading, Small Noise, $\alpha > 2$* : As the noise power is approaching zero, we have

$$Z_f(T) = 1 - \frac{1 - e^{-\rho(\alpha)T^{2/\alpha}R_f^2}}{\rho(\alpha)T^{2/\alpha}R_f^2} + \frac{\mu\sigma^2 R_f^\alpha (\Gamma(1 + \frac{\alpha}{2}) - \Gamma(1 + \frac{\alpha}{2}, R_f^2))}{P_f [\rho(\alpha)]^{\alpha/2+1} T^{\alpha/2}} + o(\sigma^2). \quad (32)$$

When $\sigma^2 = 0$, we further get

$$Z_f(T) = 1 - \frac{1 - e^{-\rho(\alpha)T^{2/\alpha}R_f^2}}{\rho(\alpha)T^{2/\alpha}R_f^2}, \quad (33)$$

and the mean achievable rate is

$$\tau_f = \frac{1}{\rho(\alpha)R_f^2} \int_0^\infty \frac{1 - e^{-\rho(\alpha)(e^t-1)^{2/\alpha}R_f^2}}{(e^t-1)^{2/\alpha}} dt. \quad (34)$$

3) *Special Case When Interference Experiences Rayleigh Fading*: For Rayleigh fading, the results are essentially the same as that in the general fading case. The only additional simplification is the evaluation of $\rho(\alpha)$. We just give the result in the very special case when $\sigma^2 = 0$ and $\alpha = 4$.

When the interference experiences Rayleigh fading, we have $\mathbb{E}_g(g^{\frac{1}{2}}) = \mu \int_0^\infty g^{\frac{1}{2}} e^{-\mu g} dg = (1/2) \cdot \sqrt{\pi/\mu}$, and consequently,

$$\rho(4) = \frac{\pi^2}{2} \left(\lambda'_m \sqrt{\frac{WP_m}{P_f}} + \lambda'_f W \right). \quad (35)$$

The SINR distribution is then given by

$$Z_f(T) = 1 - \frac{1 - e^{-\rho(4)\sqrt{T}R_f^2}}{\rho(4)\sqrt{T}R_f^2}. \quad (36)$$

The mean achievable rate is simplified into

$$\begin{aligned} \tau_f &= \int_0^\infty \frac{1 - e^{-\rho(4)R_f^2\sqrt{e^t-1}}}{\rho(4)R_f^2\sqrt{e^t-1}} dt \\ &= 2 \int_0^\infty \frac{1 - e^{-y}}{y^2 + \rho^2(4)R_f^4} dy. \end{aligned} \quad (37)$$

These expressions are convenient for numerical evaluation.

C. Mean Achievable Rates of Nonsubscribers and Subscribers

There are two types of nonsubscribers: those outside nonsubscribers who access MBSs and those inside nonsubscribers who access FAPs. When the number of outside nonsubscribers in a macrocell is no greater than the total number of subchannels (i.e., $U_{\text{out}} \leq M$), each nonsubscriber

UE exclusively occupies a subchannel, and its mean achievable rate is τ_m . However, when $U_{\text{out}} > M$, those U_{out} UEs share the M subchannels with mean achievable rate $\frac{M}{U_{\text{out}}}\tau_m$. Since the evaluation is conditioned upon the existence of at least one UE, the mean achievable rate of an outside nonsubscriber UE is given by

$$\tau_{\text{out}} = \frac{\sum_{i=1}^M \mathbb{P}\{U_{\text{out}} = i\} + \sum_{i=M+1}^{\infty} \mathbb{P}\{U_{\text{out}} = i\} \frac{M}{i}}{1 - \mathbb{P}\{U_{\text{out}} = 0\}} \tau_m. \quad (38)$$

Similarly, the mean achievable rate of an inside nonsubscriber is given by

$$\tau_{\text{in}} = \frac{\sum_{j=1}^{M_s} \mathbb{P}\{U_{\text{in}} = j\} + \sum_{j=M_s+1}^{\infty} \mathbb{P}\{U_{\text{in}} = j\} \frac{M_s}{j}}{1 - \mathbb{P}\{U_{\text{in}} = 0\}} \tau_f. \quad (39)$$

When averaged over both inside and outside nonsubscribers, the overall mean achievable rate of nonsubscriber is obtained as

$$\tau_n = \frac{\lambda_{\text{out}}\tau_{\text{out}} + \lambda_f\lambda_{\text{in}}\pi R_f^2\tau_{\text{in}}}{\lambda_{\text{out}} + \lambda_f\lambda_{\text{in}}\pi R_f^2}. \quad (40)$$

Regarding subscribers, note that they are exclusively served by FAPs. Similar to the analysis of nonsubscribers, the mean achievable rate of a subscriber is given by

$$\tau_s = \frac{\sum_{i=1}^{M_r} \mathbb{P}\{U_s = i\} + \sum_{i=M_r+1}^{\infty} \mathbb{P}\{U_s = i\} \frac{M_r}{i}}{1 - \mathbb{P}\{U_s = 0\}} \tau_f. \quad (41)$$

V. NUMERICAL RESULTS

The numerical results are obtained according to both the analytical results we have derived and Monte Carlo simulation. The default configurations of system model are as follows. The total number of subchannels is $M = 20$ and the coverage radius of each femtocell is $R_f = 10\text{m}$. The transmit power of an FAP is set as $P_f = 13\text{dBm}$ and that of an MBS $P_m = 39\text{dBm}$. We set the path loss exponent as $\alpha = 4$, with interference links experiencing Rayleigh fading. The wall penetration loss is set as $W = -6\text{dB}$. We focus on the interference-limited regime, and for simplicity we ignore the noise power (i.e., $\sigma^2 = 0$). The density of MBSs is set as $\lambda_m = 0.00001$ and of FAPs $\lambda_f = 0.0001$. So the average coverage area of an MBS is roughly equal to a circle with a radius of 180m, and on average there are ten FAPs within the coverage area of an MBS. Unless otherwise specified, the subscribers and inside nonsubscribers are distributed within an FAP coverage area with intensities $\lambda_s = \lambda_{\text{in}} = 0.015$. The intensity of outside nonsubscribers is set as $\lambda_{\text{out}} = 0.0001$. So on average, each femtocell contains about 10 subscribers and inside nonsubscribers, and each macrocell contains about 10 outside nonsubscribers. Note that due to

statistical fluctuations, the number of UEs may occasionally exceeds the number of available subchannels.

Figure 4 displays the SINR distributions of macrocell UEs and femtocell UEs, when the number of shared subchannels is set as $M_s = 10$. We plot in dotted curves the analytical results, and we also plot the empirical cdfs obtained from Monte Carlo simulation. The curves reveal that the simulation results match the analytical results well, thus corroborating the accuracy of our theoretical analysis. From the SINR distributions, we observe that while the macrocell UEs experience a fair amount of interference, due to the shrinking cell size, the interference for femtocell UEs is substantially alleviated.

Figure 5 displays the mean achievable rates of macrocell UEs and femtocell UEs. In Figure 5(a) the performance is shown as the FAP intensity λ_f increases. We observe that the mean achievable rates of both macrocell and femtocell UEs only mildly decrease with the increasing of λ_f , suggesting that the network may robustly tolerate the deployment of FAPs. In Figure 5(b) the performance is shown as the outside nonsubscribers intensity λ_{out} increases. We observe that the mean achievable rates of macrocell and femtocell UEs drop initially and then tend to be stable. This is because the rise of the number of outside nonsubscribers results in more subchannels in use at each MBS, which brings more interference to the network. However, when the density of outside nonsubscribers is large enough, almost all the subchannels of the MBSs are used and the UEs are served by time-sharing with equal time proportion. In this case, the interference will not increase any more with the rise of the density of outside nonsubscribers. Therefore, for an active UE, the mean rate tends to be stable.

Figure 6 gives the mean achievable rates of macrocell UEs and femtocell UEs under various transmission powers. From Figure 6(a), we see that as the transmission power of the FAPs increases, the rate of femtocell UEs increases correspondingly. However, the increasing power of the FAPs will impose more interference to the macrocell UEs and degrade the performance of them. Figure 6(b) shows that when fixing the power of FAPs and increasing the power of MBSs, the performance of femtocell UEs deteriorates seriously.

Figure 7 gives the performance of nonsubscribers and subscribers under various numbers of shared subchannels in an FAP. The mean achievable rate of nonsubscribers is the average over both outside and inside nonsubscribers. When M_s is small, which is the case that few subchannels are shared by each FAP, the mean rate of nonsubscribers is terrible although the

performance of subscribers is pretty good. As the number of shared subchannels increases, the performance of nonsubscribers improves and of subscribers decreases, which is consistent with the actual. At the extreme case that almost all subchannels are shared to the nonsubscribers, the performance of subscribers deteriorates severely. This picture gives an evidence of the conflict between performance of subscribers and nonsubscribers. A compromise must be taken between the performance of both kinds of UEs. According to Figure 7, at the default configuration, it is advisable to choose the value of M_s in the range of $[7, 12]$. The result indicates that within a large range of the value M_s , the performance is pretty good.

Figure 8 shows the mean achievable rate of nonsubscribers and subscribers under different proportions of inside nonsubscribers and subscribers in femtocells. The sum density of all kinds of UEs in a femtocell is fixed, which is $\lambda_s + \lambda_{in} = 0.03$. Figure 8(a) gives the performance in the case when most of the femtocell UEs are nonsubscribers while Figure 8(b) gives the opponent case. The results indicate that in order to achieve a good performance for both kinds of UEs, the shared number of subchannels in each FAP should changed with the density of the inside nonsubscribers.

VI. CONCLUSIONS

This paper has proposed a tractable network model to evaluate the tradeoff between the nonsubscribers and subscribers. We derived the closed form expressions of the SINR distribution and the mean achievable rate for each UE. In the special cases, we saw that the expressions can be simplified into some quite concise forms. With these closed form results, the relationship between the performance of each US and the proportion of shared resource became clear.

The numerical results show that there is an apparent conflict between the performance of nonsubscribers and that of subscribers. The increase of the shared resource will lead to the improve of the performance of nonsubscribers, but the performance of subscribers will deteriorate. Moreover, it is shown that the amount of shared spectrum has a large value space in order to balance the performance of both nonsubscribers and subscribers.

APPENDIX A

Let r be the distance between an outside nonsubscriber and its serving MBS. Since an outside nonsubscriber always chooses its nearest MBS to access, the cdf of r is obtained by

$$\begin{aligned}\mathbb{P}\{r \leq R\} &= 1 - \mathbb{P}\{\text{no MBS closer than } R\} \\ &= 1 - e^{-\lambda_m \pi R^2}.\end{aligned}\quad (42)$$

Then, the pdf of r is given by

$$f(r) = e^{-\lambda_m \pi r^2} 2\pi \lambda_m r. \quad (43)$$

Having the pdf of r , we derive the cdf of SINR and the mean achievable rate for an outside nonsubscriber UE. Assuming that the considered UE is at distance r from its serving MBS, g is the fading of an interference link, and R is the distance between the UE and an interfering access point, the SINR experienced by the UE is given by $\text{SINR} = \frac{P_m h r^{-\alpha}}{I_c + I_f + \sigma^2}$, where $I_c = \sum_{i \in \Phi'_m \setminus \{b_0\}} P_m g_i R_i^{-\alpha}$ is the interference from the macrocell tier (excluding the serving MBS itself which is denoted by b_0) and $I_f = \sum_{j \in \Phi'_f} W P_f g_j R_j^{-\alpha}$ is the interference from the femtocell tier with the wall penetration loss taken into account.

We can thus derive the cdf of the SINR following

$$\begin{aligned}Z_m(T) &= 1 - \mathbb{P}\{\text{SINR} > T\} \\ &= 1 - \int_0^\infty 2\pi \lambda_m r e^{-\pi \lambda_m r^2} \mathbb{P}\left\{\frac{P_m h r^{-\alpha}}{I_c + I_f + \sigma^2} > T\right\} dr \\ &= 1 - \int_0^\infty 2\pi \lambda_m r e^{-\pi \lambda_m r^2} \mathbb{P}\left\{h > \frac{T r^\alpha}{P_m} (I_c + I_f + \sigma^2)\right\} dr \\ &= 1 - \int_0^\infty 2\pi \lambda_m r e^{-\pi \lambda_m r^2} \mathbb{E}\left(\exp\left(-\frac{\mu T r^\alpha}{P_m} (I_c + I_f + \sigma^2)\right)\right) dr \\ &= 1 - \int_0^\infty 2\pi \lambda_m r e^{-\pi \lambda_m r^2 - \mu T r^\alpha \sigma^2 / P_m} \mathcal{L}_{I_c + I_f}\left(\frac{\mu T r^\alpha}{P_m}\right) dr.\end{aligned}\quad (44)$$

By the definition of Laplace transform we get

$$\begin{aligned}
\mathcal{L}_{I_c+I_f}(s) &= E_{I_c+I_f}\left(e^{-s(I_c+I_f)}\right) \\
&= E_{\Phi'_m}\left(\exp\left(-s\sum_{i\in\Phi'_m\setminus\{b_0\}}P_m g_i R_i^{-\alpha}\right)\right)E_{\Phi'_f}\left(\exp\left(-s\sum_{j\in\Phi'_f}W P_f g_j R_j^{-\alpha}\right)\right) \\
&= E_{\Phi'_m}\left(\prod_{i\in\Phi'_m\setminus\{b_0\}}E_{g_i}\left(\exp\left(-s g_i R_i^{-\alpha} P_m\right)\right)\right)E_{\Phi'_f}\left(\prod_{j\in\Phi'_f}E_{g_j}\left(\exp\left(-s g_j R_j^{-\alpha} W P_f\right)\right)\right) \\
&= E_{\Phi'_m}\left(\prod_{i\in\Phi'_m\setminus\{b_0\}}\mathcal{L}_g(s R_i^{-\alpha} P_m)\right)E_{\Phi'_f}\left(\prod_{j\in\Phi'_f}\mathcal{L}_g(s R_j^{-\alpha} W P_f)\right) \\
&= \exp\left(-2\pi\lambda'_m\int_r^\infty(1-\mathcal{L}_g(sv^{-\alpha}P_m))v dv\right)\times \\
&\quad \exp\left(-2\pi\lambda'_f\int_0^\infty(1-\mathcal{L}_g(sw^{-\alpha}W P_f))w dw\right), \tag{45}
\end{aligned}$$

where the last equality follows from the pgf of PPP [?]. Next let us evaluate (A) and (B) respectively.

$$\begin{aligned}
(A) &= \int_r^\infty \int_0^\infty (1 - e^{-sv^{-\alpha}P_m g})f(g)v dg dv \\
&= \int_0^\infty \left(\int_r^\infty (1 - e^{-sv^{-\alpha}P_m g})v dv\right)f(g)dg. \tag{46}
\end{aligned}$$

Let $y = v^{-\alpha}$, then $v = y^{-\frac{1}{\alpha}}$, so we get

$$(A) = \frac{1}{\alpha} \int_0^\infty \left(\int_0^{r^{-\alpha}} (1 - e^{-sP_m g y})y^{-\frac{2}{\alpha}-1} dy\right)f(g)dg.$$

Integrating by parts, since $y^{-\frac{2}{\alpha}-1}dy = -\frac{\alpha}{2}dy^{-\frac{2}{\alpha}}$, we obtain

$$(A) = \frac{1}{\alpha} \int_0^\infty \left(\left(1 - e^{-sP_m g y}\right)y^{-\frac{2}{\alpha}}\left(-\frac{\alpha}{2}\right)\Big|_0^{r^{-\alpha}} - \int_0^{r^{-\alpha}} sP_m g e^{-sP_m g y}y^{-\frac{2}{\alpha}}\left(-\frac{\alpha}{2}\right)dy\right)f(g)dg$$

We have assumed $\alpha > 2$, so $\lim_{y \rightarrow 0}(1 - e^{-sP_m g y})y^{-\frac{2}{\alpha}} = 0$. Letting $t = sP_m g y$, we obtain

$$\begin{aligned}
(A) &= \frac{1}{2} \int_0^\infty \left(-\left(1 - e^{-sP_m g r^{-\alpha}}\right)r^2 + (sP_m g)^{\frac{2}{\alpha}} \int_0^{sP_m g r^{-\alpha}} e^{-t}t^{1-\frac{2}{\alpha}-1} dy\right)f(g)dg \\
&= -\frac{r^2}{2} + \frac{r^2}{2}\mathcal{L}_g(sP_m r^{-\alpha}) + \frac{1}{2}(sP_m)^{\frac{2}{\alpha}} \int_0^\infty g^{\frac{2}{\alpha}} \left(\Gamma\left(1 - \frac{2}{\alpha}\right) - \Gamma\left(1 - \frac{2}{\alpha}, sP_m g r^{-\alpha}\right)\right)f(g)dg.
\end{aligned}$$

From the properties of Gamma function, we have

$$\begin{aligned}\Gamma\left(1 - \frac{2}{\alpha}\right) &= -\frac{2}{\alpha}\Gamma\left(-\frac{2}{\alpha}\right) \\ \Gamma\left(1 - \frac{2}{\alpha}, sP_m g r^{-\alpha}\right) &= (sP_m g r^{-\alpha})^{-2/\alpha} e^{-sP_m g r^{-\alpha}} - \frac{2}{\alpha}\Gamma\left(-\frac{2}{\alpha}, sP_m g r^{-\alpha}\right),\end{aligned}$$

so that (A) can be simplified as

$$(A) = -\frac{r^2}{2} + \frac{1}{\alpha}(sP_m)^{\frac{2}{\alpha}}\mathbb{E}_g\left(g^{\frac{2}{\alpha}}\left(\Gamma\left(-\frac{2}{\alpha}, sP_m g r^{-\alpha}\right) - \Gamma\left(-\frac{2}{\alpha}\right)\right)\right).$$

The evaluation of (B) is almost the same, and we have

$$(B) = -\frac{1}{\alpha}(sWP_f)^{\frac{2}{\alpha}}\Gamma\left(-\frac{2}{\alpha}\right)\mathbb{E}_g\left(g^{\frac{2}{\alpha}}\right).$$

Substituting (A) and (B) into $\mathcal{L}_{I_c+I_f}(s)$ and rearranging terms in $Z_m(T)$ hence leads to (9).

Now we evaluate the mean achievable rate. Since for a positive random variable X , $\mathbb{E}[X] = \int_{t>0} \mathbb{P}\{X > t\} dt$, we have

$$\begin{aligned}\tau_m &= E[\ln(1 + \text{SINR})] \\ &= \int_0^\infty e^{-\pi\lambda_m r^2} \mathbb{E}\left[\ln\left(1 + \frac{P_m h r^{-\alpha}}{I_c + I_f + \sigma^2}\right)\right] 2\pi\lambda_m r dr \\ &= \int_0^\infty e^{-\pi\lambda_m r^2} \int_0^\infty \mathbb{P}\left\{\ln\left(1 + \frac{P_m h r^{-\alpha}}{I_c + I_f + \sigma^2}\right) > t\right\} dt 2\pi\lambda_m r dr \\ &= \int_0^\infty e^{-\pi\lambda_m r^2} \int_0^\infty \mathbb{P}\left\{h > \frac{r^\alpha}{P_m}(I_c + I_f + \sigma^2)(e^t - 1)\right\} dt 2\pi\lambda_m r dr \\ &= \int_0^\infty e^{-\pi\lambda_m r^2} \int_0^\infty \mathbb{E}\left(e^{-\mu \frac{r^\alpha}{P_m}(I_c + I_f + \sigma^2)(e^t - 1)}\right) dt 2\pi\lambda_m r dr \\ &= \int_0^\infty \int_0^\infty e^{-\pi\lambda_m r^2 - \frac{\mu r^\alpha \sigma^2}{P_m}(e^t - 1)} \mathcal{L}_{I_c+I_f}\left(\frac{\mu r^\alpha (e^t - 1)}{P_m}\right) dt 2\pi\lambda_m r dr.\end{aligned}\quad (47)$$

From the derivation of $Z_m(T)$ we have already obtained the expression of $\mathcal{L}_{I_c+I_f}\left(\frac{\mu r^\alpha (e^t - 1)}{P_m}\right)$. When substituting into (47), we arrive at (10) and thus establish Theorem 1.

APPENDIX B

Let r be the distance between a femtocell UE and its serving FAP. Because the femtocell UEs are uniformly distributed in the circular coverage area of radius R_f of each FAP, the pdf of r is given by $f(r) = 2r/R_f^2$.

Denote by I'_c and I'_f the interference strengths from the macrocell tier and the femtocell tier respectively. Similar to the proof of Theorem 1, we have

$$Z_f(T) = 1 - \int_0^{R_f} \frac{2r}{R_f^2} e^{-\frac{\mu T r^\alpha \sigma^2}{P_f}} \mathcal{L}_{I'_c+I'_f} \left(\frac{\mu T r^\alpha}{P_f} \right) dr. \quad (48)$$

Following the same procedure as in the derivation of (45), we get the Laplace transform of $I'_c + I'_f$ as

$$\begin{aligned} \mathcal{L}_{I'_c+I'_f}(s) &= E_{I'_c+I'_f} \left(e^{-s(I'_c+I'_f)} \right) \\ &= \exp \left(-2\pi\lambda'_m \int_0^\infty (1 - \mathcal{L}_g(sv^{-\alpha}WP_m))v dv - 2\pi\lambda'_f \int_0^\infty (1 - \mathcal{L}_g(sw^{-\alpha}W^2P_f))w dw \right) \\ &= \exp \left(-\pi s^{\frac{2}{\alpha}} \Gamma \left(1 - \frac{2}{\alpha} \right) (\lambda'_m (WP_m)^{\frac{2}{\alpha}} + \lambda'_f (W^2P_f)^{\frac{2}{\alpha}}) \mathbb{E}_g \left(g^{\frac{2}{\alpha}} \right) \right). \end{aligned} \quad (49)$$

In the above, it is noteworthy that the interference from an FAP penetrates two walls thus the loss becoming W^2 instead of W . Substituting (49) into (48) with $v = r^2$, we get the SINR distribution in Theorem 2. Similar to (47), the mean achievable rate is given by

$$\tau_f = \int_0^{R_f} \int_0^\infty e^{-\frac{\mu r^\alpha \sigma^2}{P_f}(e^t-1)} \mathcal{L}_{I'_c+I'_f} \left(\frac{\mu r^\alpha (e^t-1)}{P_f} \right) \frac{2r}{R_f^2} dt dr. \quad (50)$$

Substituting (49) into (50), we get the mean achievable rate in Theorem 2.

TABLE I
SYSTEM PARAMETERS

Symbol	Description	Value
Φ_m, Φ_f	PPPs defining the MBSs and FAPs	N/A
λ_m	Density of MBSs	0.00001 MBS/m ²
λ_f	Density of FAPs	0.0001 FAP/m ²
R_f	Radius of femtocell	10m
λ_{out}	Densities of outside nonsubscribers	0.0001 user/m ²
λ_s, λ_{in}	Densities of subscribers and inside nonsubscribers	0.015 user/m ²
P_m, P_f	Transmit power at MBS and FAP	39dBm, 13dBm
M	Number of subchannels at each access point	20
M_s, M_r	Number of subchannels shared and reserved by each femtocell	Not fixed
α	Path loss exponent	4
P_{busy}^m, P_{busy}^f	Probabilities that a given subchannel is used by an MBS and an FAP	Not fixed
Φ'_m, Φ'_f	PPPs defining the MBSs and FAPs that interfere a given subchannel	N/A
λ'_m, λ'_f	Densities of MBSs and FAPs that interfere a given subchannel	Not fixed
U_{out}, U_{in}	Numbers of nonsubscribers that access a given MBS and a given FAP	Not fixed
U_s	Numbers of subscribers that access a given FAP	Not fixed
τ_f, τ_m	Mean achievable rates of femtocell UEs and macrocell UEs	Not fixed
τ_s, τ_n	Mean achievable rates of subscribers and nonsubscribers	Not fixed

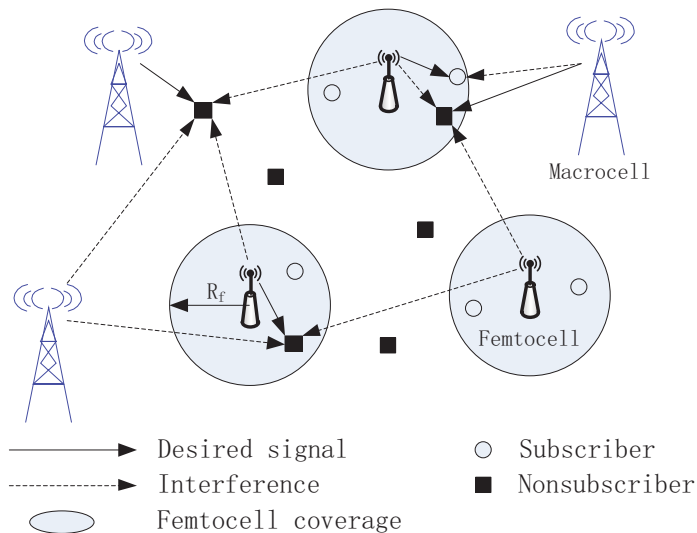


Fig. 1. Downlink two-tier network model for hybrid access femtocell.

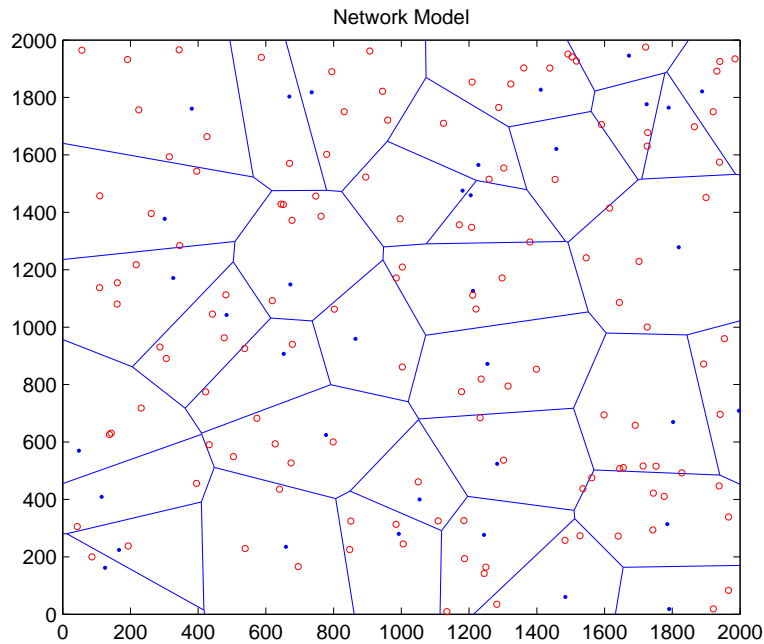


Fig. 2. The Voronoi network model. Each Voronoi cell is the coverage of a macrocell and each small circle stands for a femtocell.

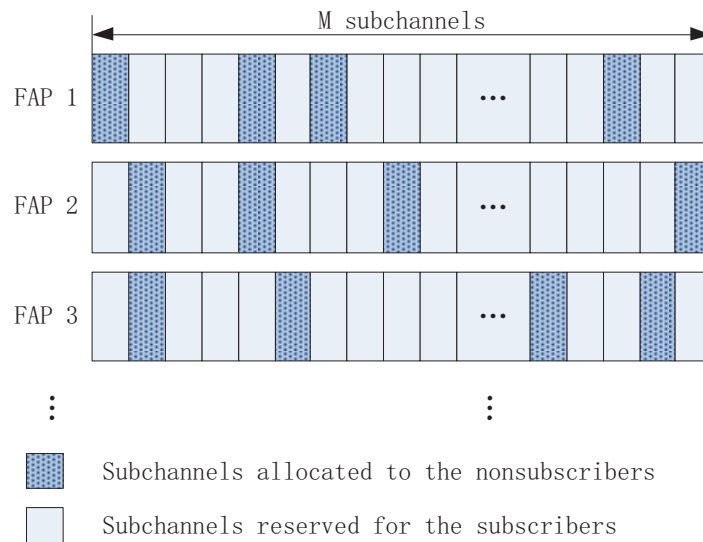


Fig. 3. Spectrum allocation in each hybrid access femtocell. All the M_s shared subchannels are randomly selected in each FAP.

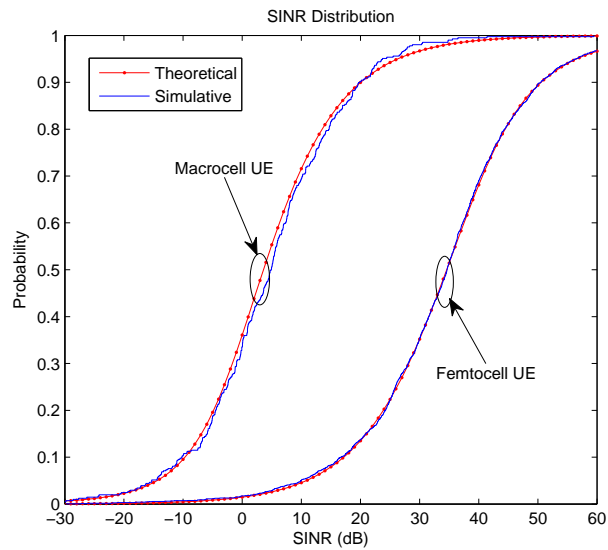
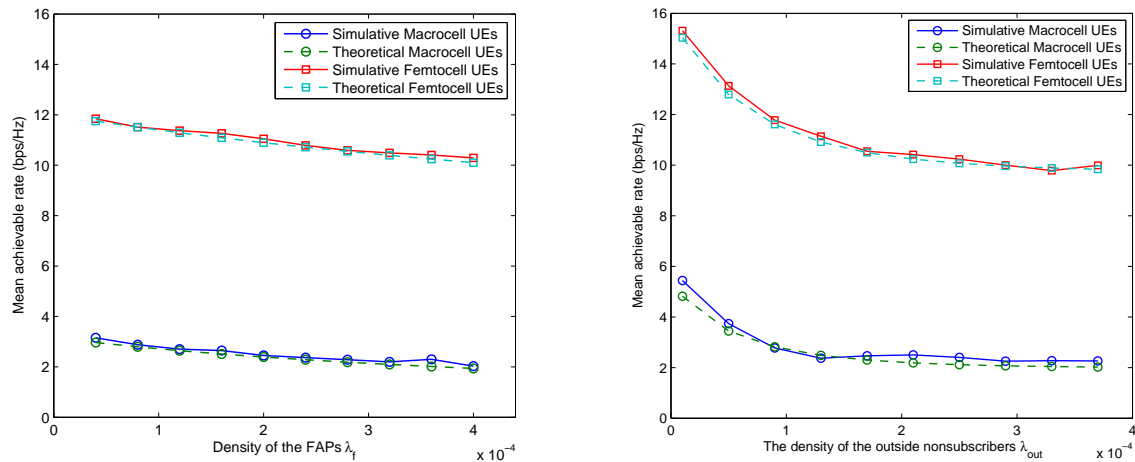


Fig. 4. Cdf of SINR for macrocell UEs and femtocell UEs when $M_s = 10$. Other parameters are set as default.



(a) Change the density of the FAPs λ_f .

(b) Change the density of outside nonsubscribers λ_{out} .

Fig. 5. Performance contrast between macrocell UEs and femtocell UEs with various densities of FAPs and outside nonsubscribers.

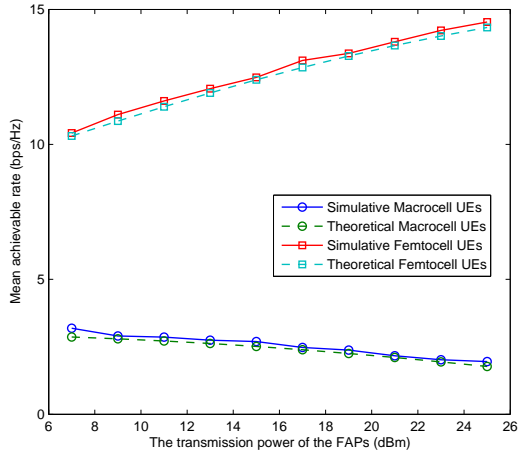
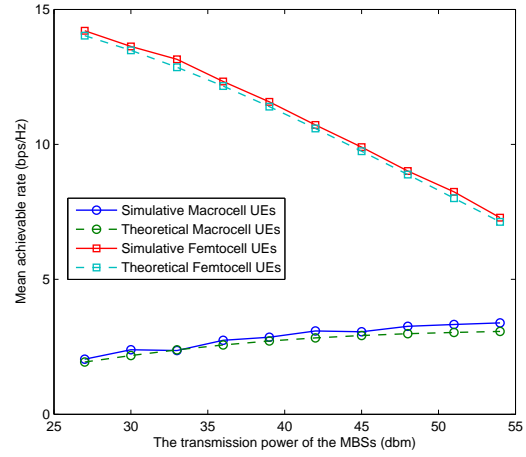
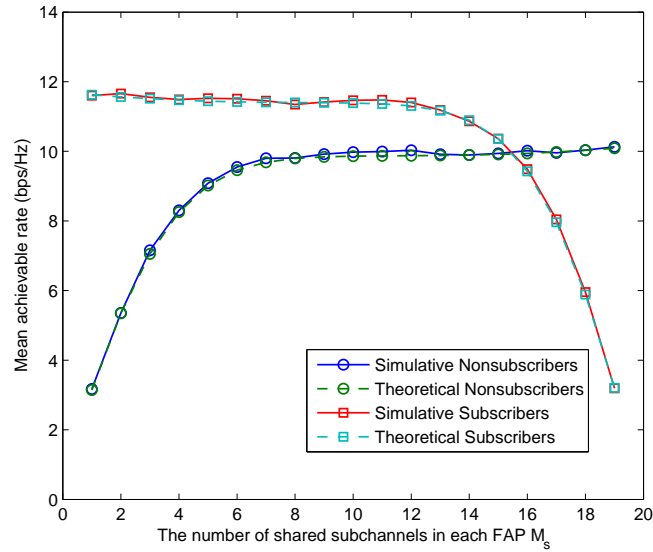
(a) Change P_f while $P_m = 39\text{dBm}$.(b) Change P_m while $P_f = 13\text{dBm}$.

Fig. 6. Performance contrast between macrocell UEs and femtocell UEs with various transmission powers.

Fig. 7. Performance of nonsubscribers and subscribers with various numbers of shared subchannels M_s in an FAP. Other parameters are set as default.

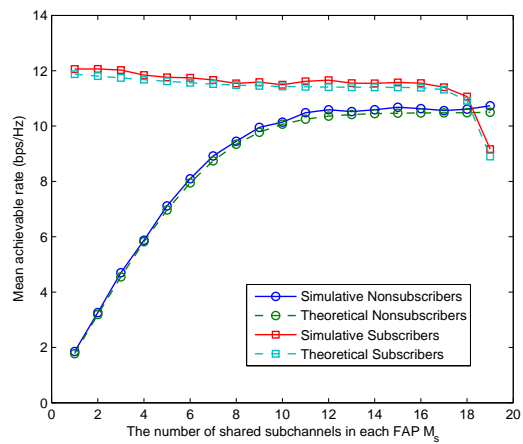
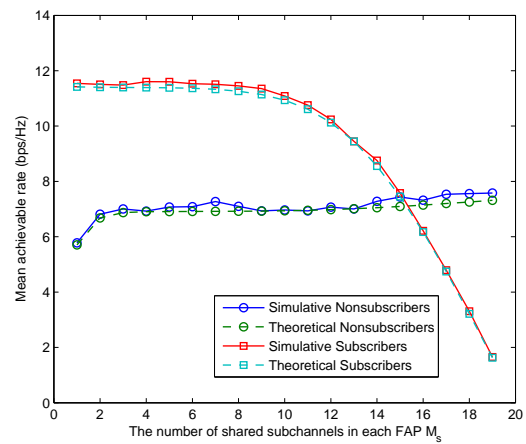
(a) $\lambda_s = 0.003$ and $\lambda_{in} = 0.027$.(b) $\lambda_s = 0.027$ and $\lambda_{in} = 0.003$.

Fig. 8. Performance contrast between nonsubscribers and subscribers with different proportions of inside nonsubscribers and subscribers.